

## Response to referee

We thank the anonymous referee for the suggestions and we are happy to say that we have been able to incorporate most of them. The number of figures have been reduced from 14 to 10 in the revised manuscript. Additionally, we proof read the final manuscript and made some slight modifications to the text in order to make it clearer. All the modifications were done using track changes. A copy of the track changed document is uploaded along with the final manuscript. Point-by-point answers to the referee's comments are below.

**Line 34: Surely also, in addition to / regardless of climate change, flooding in itself is a current threat that this paper is relevant to.**

That is absolutely correct. Including the climate change aspect in the description implies that the situation of floods may worsen in the future, and satellite based precipitation estimates can be the solution for real-time flood forecasting. The new line reads as:

*With the threats of climate change looming large, high quality precipitation products (in terms of accuracy, spatial and temporal resolution) are the need of the hour to analyse hydro-meteorological processes in real time.*

**Line 70: TMPA acronym is first expanded at line 181, please expand here at first use**  
TMPA acronym has been expanded in line 70.

**Line 103: this should be updated to “two flood prone basins”, in this revision**

We revised the text to clearly state two flood prone basins along with their names (line 103-107). The revised line reads:

*Finally, we used a macroscale hydrologic model (Variable Infiltration Capacity (VIC)) to evaluate TRMM and IMERG over two flood prone basins in Eastern India (Hirakud catchment of the Mahanadi River basin and Wainganga catchment of the Godavari River basin) for the year 2014.*

**Line 223-224: Do the authors have a reference for the Thiessen Polygon method?**

We added a reference (Schumann, 1998) for Thiessen Polygon method (line 224-226 in revised manuscript).

**Line 419-420: Lots of false alarms at very high rainfall thresholds implies that it is not good at capturing the extremes; this could have implications for flood modelling etc. and I expected to see this mentioned in the discussions / conclusions, particularly as the authors go on to complete a rainfall-runoff modelling exercise and find that the peak flows are not captured well. This should be an interesting point to mention.**

We mentioned the point in conclusion #4 in the revised manuscript (line 513-518). The line reads as below:

*At very high rainfall thresholds (>95 percentile), TRMM exhibited high false alarm ratio (FAR), especially in the North-eastern and Southern basins, implying that they do not capture the extreme precipitation magnitudes well. This was also seen in the rainfall-runoff exercise*

*where the peak flows were underpredicted in Mahanadi and Wainganga River basins, both in the case of TRMM and IMERG.*

**Lines 477-478: The authors refer to a negative bias showing overprediction - it is not clear if underprediction is really what is meant, as the bias is negative. Please clarify in the text, or check that you have positive biases for overprediction, and negative biases for underprediction, to be consistent with the biases presented earlier in the paper.**

This was a typo. We changed “overprediction” to “underprediction” in the revised manuscript (line 480). Thank you for pointing it out.

**Conclusion 7: Looking at the hydrographs, the results with IMERG and TRMM are pretty similar regardless of the calibration, for both basins. Neither are capable of capturing the peak flows, despite the results finding that precipitation is generally improved in IMERG. Could the problem be more due to the hydrological model used (would a different model perhaps result in better prediction of the peaks using either of the rainfall datasets?) rather than the choice between TRMM or IMERG? Or is it the case that the rainfall datasets cannot capture the extreme rainfall? A possible limitation that could be interesting to mention.**

Thank you for pointing this out. We added the following text to point #7 of conclusion (line 534-539).

*It will also be useful to see if other hydrologic models can capture peak flows more accurately when forced with TRMM/IMERG in Mahanadi and Wainganga basins. This would mean that the poor representation of peak flows is a function of model structural uncertainty, and not the satellite precipitation products driving the model. This will make a very interesting future case study.*

**Line 536: ‘Post forecast data assimilation scheme’ - do the authors refer to postprocessing?**

Yes, we refer to postprocessing. We clarified it in the revised manuscript and included a reference (Ye et al., 2014) for it (line 546-549).

**Figure 5: From the authors’ response, I accept that the contrast may be hard to see using a colour scale with only 1 colour. I still find this figure very hard to interpret. Perhaps it would be possible to use cool colours (blue to pink) for positive correlation, and warm (orange and red) for negative correlation? This would allow the use of more colours to avoid the contrast issue, would allow the basins with negative correlation to stand out further making the plot easier to interpret, and would avoid the use of green and red on the same figure (which it is generally recommended to avoid, due to the % of the population who are colourblind).**

We agree that the figure is not best suited for color blind people. As advised by the reviewer, we revised the colorbar of figure 5, using warm colors (variants of brown) for low correlation and cool colors (variants of blue). The new figure is placed below for illustration.

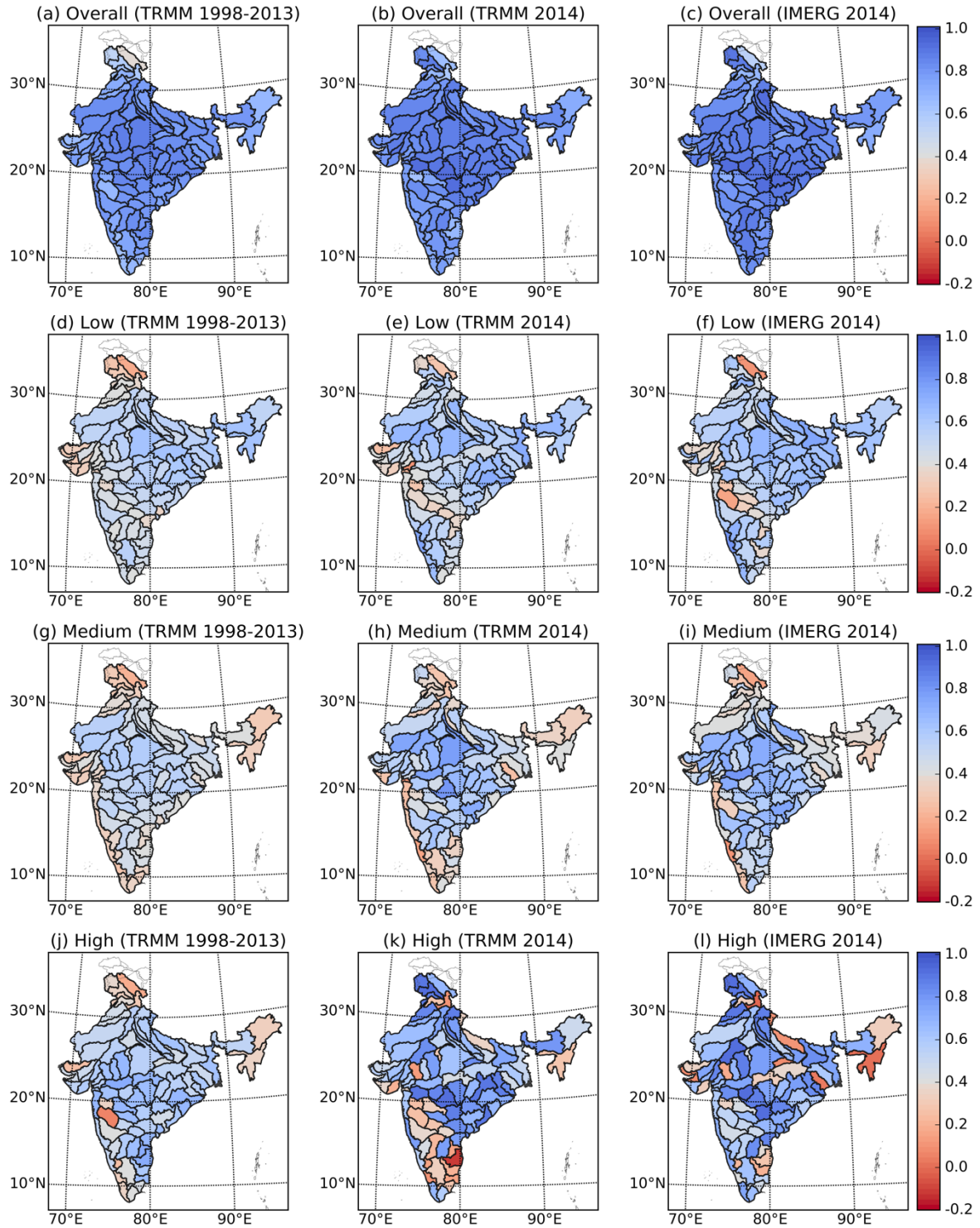


**Figure 5.** Spatial representation of correlation of TRMM (1998-2013), TRMM (2014) and IMERG (2014) over 86 delineated river basins across India for (a) – (c) overall time series, (d) – (f) low, (g) – (i) medium and (j) – (l) high rainfall regime.

**Figures 7 & 8:** Indeed, I agree with the authors comment regarding the use of two colours, I had not realised this point about the  $FAR > 0.5$ . Perhaps the relevance of  $FAR > 0.5 / POD < 0.5$  could be mentioned in table 3.

We did not mention the significance of  $FAR < 0.5$  or  $POD > 0.5$  in table 3 as defining 0.5 as a threshold for low or high POD/FAR seems arbitrary.

**Figures 9-12: These plots are discussed briefly in the manuscript; while the results are interesting, I don't think the discussion warrants four 4-panel figures. The results presented in section 3.5 are clear without needing to refer to the figures, and I would recommend moving them to the supplementary material.**

Figures 9-12 have been moved to supplementary material (Figs. S4-S7).

**Figures S1 - S3: The points on these figures should not be joined with a continuous line, as these are not continuous data; this can be difficult to interpret and can be misleading.**

Continuous lines have been removed from figures S1-S3 in the revised supplementary material.

### **References:**

- Schumann, A. H.: Thiessen Polygon Thiessen polygon BT - Encyclopedia of Hydrology and Lakes, pp. 648–649, Springer Netherlands, Dordrecht , 1998.
- Ye, A., Duan, Q., Yuan, X., Wood, E. F. and Schaake, J.: Hydrologic post-processing of MOPEX streamflow simulations, J. Hydrol., 508(Supplement C), 147–156, doi:<https://doi.org/10.1016/j.jhydrol.2013.10.055>, 2014.



1 **Does the GPM mission improve the systematic error component in satellite**  
2 **rainfall estimates over TRMM? An evaluation at a pan-India scale**

3 Harsh Beria<sup>1</sup>, Trushnamayee Nanda<sup>2</sup>, Deepak Singh Bisht<sup>2</sup>, Chandranath Chatterjee<sup>2</sup>

4 <sup>1</sup>[Institute of Earth Surface Dynamics, University of Lausanne, Switzerland](#)

5 <sup>2</sup>[Agricultural and Food Engineering Department, Indian Institute of Technology Kharagpur,](#)  
6 [Kharagpur, India](#)

7 *Correspondence to:* Harsh Beria ([harsh.beria@unil.ch](mailto:harsh.beria@unil.ch))

8 **Abstract.** Last couple of decades have seen the outburst of a number of satellite based  
9 precipitation products with Tropical Rainfall Measuring Mission (TRMM) as the most widely  
10 used for hydrologic applications. Transition of TRMM into Global Precipitation Mission  
11 (GPM) promises enhanced spatio-temporal resolution along with upgrades in sensors and  
12 rainfall estimation techniques. Dependence of systematic error components in rainfall  
13 estimates of Integrated Multi-satellitE Retrievals for GPM (IMERG), and their variation with  
14 climatology and topography, was evaluated over 86 basins in India for year 2014 and  
15 compared with the corresponding (2014) and retrospective (1998-2013) TRMM estimates.  
16 IMERG outperformed TRMM for all rainfall intensities across a majority of Indian basins,  
17 with significant improvement in low rainfall estimates showing smaller negative biases in 75  
18 out of 86 basins. Low rainfall estimates in TRMM showed a systematic dependence on basin  
19 climatology, with significant overprediction in semi-arid basins which gradually improved in  
20 the higher rainfall basins. Medium and high rainfall estimates of TRMM exhibited a strong  
21 dependence on basin topography, with declining skill in higher elevation basins. Systematic  
22 dependence of error components on basin climatology and topography was reduced in  
23 IMERG, especially in terms of topography. Rainfall-runoff modeling using Variable  
24 Infiltration Capacity (VIC) model over [two flood prone basins \(Mahanadi and Wainganga\)](#)  
25 revealed that improvement in rainfall estimates in IMERG didn't translate into improvement  
26 in runoff simulations. More studies are required over basins in different hydro-climatic zones  
27 to evaluate the hydrologic significance of IMERG.

28 **Keywords:** GPM, IMERG, TRMM, VIC, climatology, topography

Deleted: 2

Deleted: 1

Deleted: 1

Deleted: 1

Deleted: <sup>1</sup>Agricultural and Food Engineering Department, Indian Institute of Technology Kharagpur, Kharagpur, India .

Deleted: 2

Deleted: 93

Deleted: gmail

Deleted: com

Deleted: a

## 40 1 Introduction

41 The developing part of the world suffers from acute data shortage, both in terms of  
42 quality and quantity. A recent commentary from Mujumdar (2015) provided insights into the  
43 problems faced by the Indian hydrologic community due to the lack of willingness of the  
44 relevant governmental bodies to openly share meteorologic and hydrologic data and its meta  
45 data to the research community. With the threats of climate change, looming large, high  
46 quality precipitation products (in terms of accuracy, spatial and temporal resolution) are the  
47 need of the hour [to analyse hydro-meteorological processes in real time](#). Satellite  
48 precipitation products offer a viable alternative to gauge based rainfall estimates.

49 A number of satellite based precipitation estimates have cropped up in the past two  
50 decades, the famous ones being Climate Prediction Center morphing technique (CMORPH),  
51 Precipitation Estimation from Remotely Sensed Information Using Artificial Neural  
52 Networks (PERSIANN), PERSIANN Climate Data Record (PERSIANN-CDR), Tropical  
53 Rainfall Measuring Mission (TRMM), Asian Precipitation - Highly-Resolved Observational  
54 Data Integration Towards Evaluation (APHRODITE) and National Oceanic and Atmospheric  
55 Administration (NOAA) Climate Prediction Center (CPC). A number of studies over the past  
56 decade have evaluated the hydrologic application of these datasets over regions with varied  
57 topography and climatology.

58 Artan et al. (2007) found reasonable streamflow simulations using CPC over four  
59 basins in Africa and South-east Asia while Collischonn et al. (2008) found similar results  
60 using TRMM over Amazon River basin. Akhtar et al. (2009) used neural networks to forecast  
61 discharges at varying lead times using TRMM 3B42V6 precipitation estimates. Wu et al.  
62 (2012) used TRMM 3B42V6 estimates to develop a real-time flood monitoring system and  
63 concluded that the probability of detection (POD) improved with longer flood durations and  
64 larger affected areas. Kneis et al. (2014) evaluated TRMM 3B42-V7 and its real-time  
65 counterpart TRMM 3B42-V7RT over Mahanadi River basin in India and found the research  
66 product (3B42) to be superior to the real-time alternative (3B42RT). Peng et al. (2014) found  
67 a systematic dependence of TRMM estimates on climatology in North-West China,  
68 characterizing the wetter regions better than the drier ones. Bajracharya et al. (2014) used  
69 CPC to drive a hydrologic model over Bagmati basin in Nepal and reported that the  
70 incorporation of local rain gauge data tremendously benefited the streamflow simulations.  
71 Shah and Mishra (2015) explored uncertainty in the estimates of multiple satellite rainfall

Deleted: ing

73 products over major Indian basins. Most of the studies which evaluated multiple satellite  
74 precipitation estimates have reported TRMM to give the best estimate over the Tropical part  
75 of the world (Gao and Liu, 2013; Prakash et al., 2016b; Zhu et al., 2016).

76 Tropical Rainfall Measuring Mission (TRMM) satellite was launched in late 1997 and  
77 provides high resolution (0.25° x 0.25°) quasi-global (50° N-S) rainfall estimates (Huffman et  
78 al., 2007). The TRMM mission is a joint mission between the National Aeronautics and  
79 Space Administration (NASA) and the Japan Aerospace Exploration (JAXA) Agency to  
80 study rainfall for weather and climate research. The TRMM satellite produced 17 years of  
81 valuable precipitation data over the Tropics.

82 Owing to the tremendous success of [TRMM Multi-satellite Precipitation Analysis](#)  
83 (TMPA) mission, Global Precipitation Measurement (GPM) was launched on February 27,  
84 2014 (Liu, 2016). The GPM sensors carry first spaceborne dual-frequency phased array  
85 precipitation radar (DPR) operating at Ku (13 GHz) and Ka (35 GHz) bands and a canonical-  
86 scanning multichannel (10-183 GHz) microwave imager (GMI) (Hou et al., 2014). The  
87 improved sensitivity of Ku and Ka bands allow for improved detection of low precipitation  
88 rates (<0.5 mm/h) and falling snow.

89 A few preliminary assessments of GPM over India and China (Prakash et al., 2016a,  
90 2016b; Tang et al., 2016a) suggest an improvement over TMPA. For 2014 monsoon (Prakash  
91 et al., 2016b) reported that Integrated Multi-satellitE Retrievals for GPM (IMERG), which is  
92 a level three multi-satellite precipitation algorithm of GPM (Hou et al., 2014), outperformed  
93 TMPA in extreme rainfall detection along the Himalayan foothills in North India and over  
94 North Western India, with slightly reduced false alarms. Tang et al. (2016a) found that  
95 IMERG outperformed TMPA in almost all the indices for every sub-region of mainland  
96 China at 3-hourly and daily temporal resolutions. They also reported that IMERG reproduced  
97 probability density functions more accurately at various precipitation intensities and better  
98 represented the precipitation diurnal cycles. In another work by Prakash et al. (2016a),  
99 IMERG was compared with Global Satellite Mapping of Precipitation (GSMaP) V6 and  
100 TMPA 3B42V7 for the 2014 monsoon over India. It was found that IMERG estimates  
101 represented the mean monsoon rainfall and its variability more realistically, with fewer  
102 missed and false precipitation bias and improvements in the precipitation distribution over  
103 low rainfall rates.

104 Most of the previous studies that compared satellite and reanalysis precipitation  
105 products for pan-India focused at a grid scale, rather than a basin scale (Prakash et al., 2015,  
106 2016a, 2016b). We [followed](#) a basin scale [approach](#) as it is more relevant in terms of water  
107 resources assessment for policy makers. It provides a clear signal of the utility of the satellite  
108 precipitation products at the required spatial resolution for water managers working at a basin  
109 scale. Also, at a basin scale, the statistical and hydrologic results are more complementary  
110 (Bisht et al., 2017; Kneis et al., 2014).

Deleted: focused

Deleted: at

111 In this study, we comprehensively evaluated TRMM 3B42 from 1998-2013 over 86  
112 basins in India and explored systematic biases due to climatology and topography. We then  
113 compared TRMM 3B42 precipitation estimates with IMERG for 2014 and explored if the  
114 systematic biases were reduced in IMERG, and whether IMERG was able to better capture  
115 the low rainfall magnitudes. Finally, we used a macroscale hydrologic model (Variable  
116 Infiltration Capacity (VIC)) to evaluate TRMM and IMERG over [two](#) flood prone basins in  
117 Eastern India ([Hirakud catchment of the Mahanadi River basin and Wainganga catchment of](#)  
118 [the Godavari](#) River basin) for the year 2014.

Deleted: a

Deleted:

## 119 2 Description of the study area, datasets used and methodology

### 120 2.1 Study area

121 Water Resources Information System of India (India-WRIS) delineates India into  
122 multiple sub-basins (Fig. 1a) (India, 2014). In this study, 86 basins were used, with the five  
123 excluded basins located in the Jammu and Kashmir region of Northern India (details included  
124 in Supplementary table 1). Also, the Lakshadweep islands (located off the Indian West coast  
125 in the Arabian Sea) and the Andaman and Nicobar islands (located in the Bay of Bengal)  
126 were excluded from the analysis due to scarce rain-gauge monitoring network.

127 Most of India experiences a tropical monsoon type of climate receiving an average  
128 annual rainfall of around 1100 mm/year, of which about 70-80% is concentrated during the  
129 monsoon season (June – September). Fig. 2a shows the spatial distribution of rainfall (details  
130 in supplementary table 1), calculated using India Meteorological Department (IMD) gridded  
131 precipitation dataset (computed using 31 years (1980-2010) of rainfall time series) over India.  
132 The Western Ghats (located on the Indian West coast) and the North-Eastern basins receive  
133 the highest rainfall, with magnitudes going up to 3000 mm/year. The Western Ghats receive  
134 orographic rainfall due to steep topographic gradient that exist from the West to the East,

139 making the Eastern part a leeward area where rainfall is mainly associated with the passage  
140 of lows and depressions developed in the Bay of Bengal (Prakash et al., 2016a). Details of the  
141 orographic features of rainfall over Western Ghats can be found in Tawde and Singh (2015).  
142 The high rainfall in the North-Eastern part of India is associated with orographic control and  
143 multi-scale interactions of monsoon flow (Prakash et al., 2016a). Basins in the Indo-Gangetic  
144 plain and on the East coast receive above average rainfall of around 1400 mm/year, governed  
145 by the tropical monsoons. The North-western basins, associated with semi-arid type of  
146 climate, receive low annual rainfall ranging from 300-400 mm/year.

147 Fig. 2b shows the spatial distribution of the basin-wise elevation above mean sea level  
148 (MSL) (details in supplementary table 1). The Northern tract of Jammu and Kashmir  
149 comprises the basins with highest elevations, in between 2500 m to 5000 m above MSL.  
150 These basins suffer from scarce rain monitoring networks, due to which five of these high  
151 elevation basins have been ignored in the analysis. High Pitch Mountains are also found in  
152 the North-Eastern basins where basin-wise elevation goes as high as 1400 m above MSL. The  
153 Western Ghats are characterized by a sharp topographic gradient with the elevations  
154 increasing from around 200 m above MSL on the West coast to beyond 600 m above MSL as  
155 we move east. This transition results in heavy orographic rainfall on the West coast and leads  
156 to the sharp rainfall contrast on the leeward side of the Western Ghats.

157 Rainfall-runoff modeling was done in Hirakud catchment of the Mahanadi River  
158 basin (MRB) and Wainganga catchment of Godavari River basin. MRB, situated near the  
159 Eastern coast of India, is one of the largest Indian basins draining an area of 1,41,000 km<sup>2</sup>. It  
160 is prone to frequent flooding at the downstream, with five major flood events in the first  
161 decade of the 21st century (Jena et al., 2014). On the upstream part of the MRB is a multi-  
162 purpose dam (Hirakud) which encompasses catchment area of around 85,200 km<sup>2</sup> (Fig. 1b).  
163 Hirakud dam started its operations in 1957 and its upstream does not include any major dam,  
164 although a number of small scale irrigation reservoirs are operational during the monsoon.  
165 Agricultural, forest and shrub land account for around 55%, 35% and 7% of the total basin  
166 coverage respectively (Kneis et al., 2014). Wainganga river basin, the largest sub-basin of  
167 Godavari basin (located in Peninsular India) drains a total of 51,422 km<sup>2</sup> area. Both the  
168 basins receive annual rainfall of around 1500 mm.

## 169 2.2 Datasets used

Deleted: m.s.l

Deleted: m.s.l

Deleted: m.s.l

Deleted: m.s.l

Deleted: on

Formatted: Superscript

175           IMD gridded rainfall dataset was used as the reference product and Tropical Rainfall  
176 Measuring Mission (TRMM) and Integrated Multi-satellitE Retrievals for GPM (IMERG)  
177 were compared against IMD. A brief summary of the datasets is given in Table 1. A brief  
178 introduction to the three rainfall datasets is given below.

### 179 **2.2.1 Gridded IMD and streamflow dataset**

180           IMD gridded precipitation dataset provides daily rainfall estimates over the Indian  
181 landmass from 1901-2014 at a spatial resolution of  $0.25^\circ \times 0.25^\circ$ . It has been developed using  
182 a dense network of rain gauges consisting of 6955 stations and is known to reasonably  
183 capture the heavy orographic rainfall in the Western Ghats, the Northeast and the low rainfall  
184 on the leeward side of the Western Ghats. Details about the number of stations used to make  
185 the gridded product are discussed in the supplementary material. For a detailed discussion on  
186 the evolution of IMD gridded dataset, refer to Pai et al. (2014).

187           It is to be noted that IMD measures rainfall accumulation at 8:30 AM Indian Standard  
188 time (IST) or (3:00 AM UTC). The accumulated rainfall for the previous day is provided as  
189 the rainfall estimate for current day. For instance, IMD rainfall estimate at a gauging station  
190 for September 14<sup>th</sup>, 2014 refers to the rainfall accumulation from 8:30 AM IST (3:00 AM  
191 UTC) on September 13<sup>th</sup>, 2014 to 8:30 AM IST (3:00 AM UTC) on September 14<sup>th</sup>, 2014.  
192 Both TRMM and IMERG precipitation estimates were converted to IMD timescale.

193           The gridded daily minimum and maximum temperature was obtained from IMD at a  
194 spatial resolution of  $1^\circ \times 1^\circ$  (Srivastava et al., 2009). Daily wind speed data was obtained  
195 from coupled National Centers for Environmental Prediction (NCEP) and Climate Forecast  
196 System Reanalysis (CFSR) at a spatial resolution of  $0.5^\circ \times 0.5^\circ$ . Daily discharge data at the  
197 inflow site of the Hirakud reservoir was obtained from the State Water Resources Department  
198 (Odisha), Hirakud Dam Project, Burla, Sambalpur. Daily discharge data at Wainganga basin  
199 was obtained through WRIS-website (<http://www.india-wris.nrsc.gov.in/wris.html>).

### 200 **2.2.2 Tropical Rainfall Measuring Mission (TRMM)**

201           In order to provide high resolution precipitation dataset in real-time, the TRMM  
202 satellite was launched in late 1997 and it provides 3-hourly rainfall estimates from 1998 to  
203 the current date at a quasi-global coverage ( $50^\circ$  N-S) at a spatial resolution of  $0.25^\circ \times 0.25^\circ$   
204 (Huffman et al., 2007). Two variants of TRMM multi-satellite precipitation analysis (TMPA)  
205 are available, a real time product which is available at 3-6 hours latency and the research

206 product which is available at 2-months latency. TRMM research product makes use of rain  
207 gauge stations from Global Precipitation Climatology Centre (GPCC) to post-process the  
208 TRMM estimates, details of which can be found in Huffman et al. (2007). We used TRMM  
209 research product in this study (henceforth mentioned as TRMM).

### 210 **2.2.3 Integrated Multi-Satellite Retrievals for GPM (IMERG)**

211 IMERG is the day-1 multi-satellite precipitation algorithm for GPM which combines  
212 data from TMPA, PERSIANN, CMORPH and NASA PPS (Precipitation Processing  
213 System). For a detailed understanding of the retrieval algorithm of IMERG, refer to  
214 (Huffman et al., 2014; Liu, 2016).

215 The major advancement in GPM satellite is the improved sensitivity of sensors  
216 leading to improved detection of low precipitation rates ( $<0.5$  mm/h) and falling snow, a  
217 known shortcoming of TRMM. IMERG is available in 3 variants, (a) Early run (latency  $\sim 6$   
218 hours), (b) Late run (latency  $\sim 18$  hours) and (c) Final run (latency  $\sim 4$  months) (Liu, 2016).  
219 Each product is available at half-hourly temporal and  $0.1^\circ \times 0.1^\circ$  spatial resolution. The  
220 spatial coverage is  $60^\circ$  N-S which is planned to be extended to  $90^\circ$  N-S in the near future. We  
221 used the Final run product in our analysis.

### 222 **2.3 VIC Hydrological Model**

223 VIC is a macroscale semi-distributed hydrological model which uses a grid-based  
224 approach to quantify different hydro-meteorological processes by solving water balance and  
225 energy flux equations, specifically designed to represent the surface energy and hydrologic  
226 fluxes at varying scales (Liang et al., 1994, 1996). VIC uses multiple soil layers with variable  
227 infiltration, non-linear baseflow and addresses the sub-grid scale variability in vegetation. A  
228 stand-alone routing model (Lohmann et al., 1996) is used to generate runoff and baseflow at  
229 the outlet of each grid cell, assuming linear and time-invariant runoff transport. The land  
230 surface parameterization (LSP) of VIC is coupled with a routing scheme in which the  
231 drainage system is conceptualized by connected-stem rivers at a grid scale. The routing  
232 model extends the FDTF-ERUHDIT (First Differenced Transfer Function-Excess Rainfall  
233 and Unit Hydrograph by a Deconvolution Iterative Technique) approach (Duband et al.,  
234 1993) with a time scale separation and liberalized Saint-Venant equation type river routing  
235 model. The model assumes runoff transport process to be linear, stable and time invariant.

236 VIC has been successfully used in a number of global and local hydrologic studies  
237 (Hamlet and Lettenmaier, 1999; Shah and Mishra, 2016; Tong et al., 2014; Wu et al., 2014;  
238 Yong et al., 2012). A recent commentary on the need for process-based evaluation of large-  
239 scale hyper-resolution models by Melsen et al. (2016) provides interesting insights into the  
240 use of VIC at different spatial scales and why we shouldn't just decrease the grid size (hence  
241 increasing the spatial resolution of model) without considering the dominant processes at that  
242 scale. In lines with the discussions in Melsen et al. (2016), VIC was run at a grid size of  $0.5^\circ$   
243  $\times 0.5^\circ$  for Hirakud basin and at  $0.25^\circ \times 0.25^\circ$  for Wainganga basin.

#### 244 **2.4 Methodology**

245 All the analysis was performed at a basin scale. Basin-wise [daily](#) mean areal rainfall  
246 was calculated for all the three rainfall products (IMD, TRMM and IMERG) using Thiessen  
247 Polygon method (Schumann, 1998) for their respective periods of availability.

248 In order to statistically evaluate the precipitation products, two skill measures were  
249 used (Pearson correlation [coefficient](#) (R) and percentage bias (Pbias/bias)) along with two  
250 threshold statistics (probability of detection (POD) and false alarm ratio (FAR)). Table 2  
251 shows the contingency table and Table 3 provides a summary of the statistical indices.

252 All the statistical inferences were drawn for the overall time series, and then  
253 separately for the different rainfall regimes. Table 4 shows the criterion to segregate the  
254 rainfall time series into different components. For computing POD and FAR for different  
255 rainfall regime, a threshold is required. The 25th percentile value was selected as the  
256 threshold for low rainfall regime, 50th percentile for medium regime, 75th percentile for high  
257 rainfall regime and 95th percentile for very high rainfall regime. The statistical indices were  
258 calculated basin-wise.

259 In order to identify systematic bias in the satellite products, one meteorologic index  
260 (long term basin mean annual rainfall) and one topographic index (basin mean elevation) was  
261 computed for the 86 basins. The long term mean annual rainfall was computed using IMD  
262 gridded dataset from 1980 – 2010 (31 years). Basin mean digital elevation model (DEM) was  
263 extracted from Shuttle Radar Topography Mission (SRTM) DEM and mean elevation was  
264 obtained on a basin-wise scale.

265 Due to the limited availability of IMERG data (starting from 2014), calibration of  
266 VIC was done using an approach similar to the one used by Tang et al. (2016b). First, VIC



267 was calibrated (2000-2011) and validated (2011-2014) using gridded IMD precipitation time  
268 series. VIC was then calibrated (2000-2011) and validated (2011-2014) with TRMM  
269 precipitation time series. Further, both the IMD and TRMM calibrated models were validated  
270 with IMERG and TRMM for the year 2014 (from April 1, 2014 to December 31st, 2014).  
271 The year 2000 was used as a warm up period for the model.

272 In line with the recent discussion by McCuen (2016) on the correct usage of statistical  
273 and graphical indices to evaluate model calibration and validation, four statistical parameters  
274 (Nash Sutcliffe efficiency (NSE), Percentage bias (Pbias), coefficient of determination ( $R^2$ )  
275 and root mean square error (RMSE)) were used to evaluate the runoff simulations from VIC.  
276 Table 3 provides a summary of these indices.

Deleted: d

### 277 3 Results

278 All the TRMM statistics were obtained for two distinct periods (1998-2013 and  
279 2014). For the year 2014, the IMERG precipitation estimates were available from March 12,  
280 2014. Therefore, the TRMM statistics for the year 2014 were obtained from March 12, 2014  
281 to December 31, 2014. Henceforth, for the sake of convenience, statistics of TRMM-R refers  
282 to the time period 1998-2013, statistics of TRMM and IMERG refers to the time period  
283 March 12, 2014 to December 31, 2014.

#### 284 3.1 Scatterplots

285 Fig. 3 shows the scatterplot of IMERG and TRMM with respect to IMD precipitation  
286 combining data from all the 86 basins for the year 2014. IMERG shows better correlation in  
287 60 out of 86 basins. On looking at the scatterplots for individual basins (Fig. 4), IMERG  
288 tends to be better correlated to IMD than TRMM. It can be seen that the correlation values go  
289 as high as 0.96 for IMERG (and 0.94 for TRMM) with a very uniform spread across the 1:1  
290 line for the five best basins (Figs. 4a–e) (decided on the basis of correlation of IMERG with  
291 IMD in 2014). These basins are situated in the flat Deccan Plateau belt in South-central India  
292 (mostly concentrated in Tapi and Godavari basins). For the other five basins (Figs. 4f–j), the  
293 poor correlation is due to the gross overestimation of IMERG/TRMM over IMD. Four of  
294 these five basins are situated in the high elevation basins in Northern India, which hints at a  
295 systematic dependence of IMERG/TRMM estimates with elevation. This is explored in detail  
296 in section 3.5.

#### 297 3.2 Basin-wise correlation

299 Basin-wise correlation was computed for retrospective analysis of TRMM-R and to  
300 compare TRMM and IMERG rainfall estimates for the year 2014. Table 5 provides the  
301 summary of the number of basins where IMERG/TRMM has a higher correlation. IMERG  
302 gives better rainfall estimates in majority of basins for all rainfall regime. The decomposition  
303 of the overall time series into different rainfall regime reduces the correlation, which can be  
304 attributed to temporal smoothening in longer time series.

305 The spatial maps (Fig. 5) provide an illustration of the slight improvement of IMERG  
306 over TRMM with spatially coherent patterns. In the overall spatial maps (Figs. 5b–c), for the  
307 year 2014, TRMM and IMERG show similar skill, with IMERG capturing the rainfall  
308 slightly better in Central and Southern India. Both show similar skill in the high rainfall areas  
309 of the Western Ghats and the North Eastern basins. IMERG gives slightly better estimates in  
310 the high elevation basins in North India. There is no significant improvement in the basins  
311 located on the Eastern coast (like the Mahanadi river basin). TRMM provides slightly better  
312 estimates of rainfall in the semi-arid basins located in the North-Western part of India. It is to  
313 be noted that TRMM statistics for 2014 are much better than its retrospective statistics  
314 (TRMM-R) with spatial coherent trends.

315 The low rainfall estimates (Figs. 5d–f) over the semi-arid North Western basins are  
316 slightly better for TRMM compared to IMERG. IMERG captures low rainfall better over the  
317 Indo-Gangetic plain. Both IMERG and TRMM show similar trends over the Western Ghats,  
318 North-Eastern basins, Eastern coast and over the Deccan Plateau. IMERG doesn't capture the  
319 low rainfall regime over the Upper Indus basin (in Northern India) and over the upper Bhima  
320 and the upper Godavari basin (in the Deccan plateau belt).

321 The medium rainfall estimates (Figs. 5g–i) are best represented in Central India and  
322 over the Deccan Plateau by TRMM and IMERG. Both show similar statistics over the  
323 Western Ghats and basins in North-Eastern and Eastern coast of India. TRMM slightly  
324 outperforms IMERG in the North-Western basin of Rajasthan, a trend also found in the low  
325 rainfall regime. IMERG doesn't capture the medium rainfall trends over the Upper Indus  
326 basin (in Northern India). In general, TRMM-R medium rainfall estimates are best correlated  
327 in the semi-arid region of Rajasthan (North-Western basins) and in Central India. There is not  
328 much variability in the correlation of medium rainfall trends of TRMM-R, with correlation  
329 coefficient mostly around 0.5 for entire India, except for the high elevation Upper Indus  
330 basin.

Deleted:

Deleted: states

Deleted: (Rajasthan)

334 The high rainfall estimates (Figs. 5j-k) show highest correlation in the Deccan  
335 Plateau belt, higher elevation basins in Northern India, the Western Ghats and the East coast  
336 basins (except for the Southern-most basin) for TRMM and IMERG. High rainfall estimates  
337 of TRMM are better correlated than IMERG in the North-Eastern basins of Brahmaputra and  
338 Barak and the North-Western basins of Rajasthan. Both show similar correlation over the  
339 high elevation basins in the North and over the Western Ghats. IMERG outperforms TRMM  
340 in the rain-shadow area of the Western Ghats and in the South-Eastern basins of Pennar and  
341 Cauvery. Retrospective maps of TRMM-R (Fig. 5j) suggest that high rainfall is adequately  
342 captured in the Indo-Gangetic plain, Western Ghats, North-Western basins of Rajasthan,  
343 South-Eastern basins of Pennar and Cauvery and the Eastern coast basins of Central India.  
344 However, TRMM gives very low correlation values for the rain-shadow belt of the Western  
345 Ghats, suggesting that it doesn't capture the steep orographic gradient. The high rainfall  
346 estimates of TRMM-R give modest correlation in the North-Eastern basins, high elevation  
347 basins in Northern India and the West most basins of the South (Varrar and Periyar).

### 348 **3.3 Basin-wise bias**

349 Basin-wise bias was computed for retrospective analysis of TRMM-R and to compare  
350 TRMM and IMERG rainfall estimates for the year 2014. Bias for low rainfall regime (Fig.  
351 S2b) suggests that TRMM is more positively biased than IMERG for 75 out of 86 basins  
352 implying overestimation, which is a known problem with TRMM as its sensors cannot detect  
353 very low rainfall magnitudes ( $<0.5$  mm/hour) (Hou et al., 2014). If it detects a low intensity  
354 storm, it is most likely to overestimate (Fig. S2b). This seems to have improved in the  
355 IMERG product, due to the sensor improvements in the GPM mission (Huffman et al., 2014).  
356 The number of unbiased basins ( $-10\% \leq \text{bias} \leq 10\%$ ) increased from 28 in TRMM to 37 in  
357 IMERG basins.

358 The spatial maps for the overall rainfall time series (Figs. 6a-c) suggests similar bias  
359 patterns in TRMM and IMERG with spatial coherent trends throughout most of India.  
360 IMERG gives slightly smaller bias (closer to zero) over the high elevation basins of North  
361 India (Upper Indus basin) and slightly larger bias (more negative) over the North Eastern  
362 basins (of Brahmaputra and Barak) and the West flowing rivers of Kutch on the Western  
363 coast in the state of Gujarat. IMERG and TRMM give large positive biases (overprediction)  
364 over Upper and Middle Godavari basin (in Deccan Plateau belt) which suggests that the sharp  
365 topographic gradient is not well captured. Retrospective maps of TRMM-R suggest

366 underestimation over high elevation basins in Northern India (Indus, Jhelum and Chenab  
367 basins). However, TRMM captures the heavy precipitation on the Western Ghats well with  
368 low biases.

369 The low rainfall spatial maps (Figs. 6d–f) show large overprediction (positive bias) by  
370 TRMM (1998-2013 and 2014) which is improved in IMERG. The improvement is most  
371 prominent in the North Eastern basins (of Brahmaputra and Barak), Central India (Mahi,  
372 Chambal and the Indo-Gangetic plain), rain-shadow area of the Western Ghats and the South-  
373 Eastern coast. IMERG shows gross overprediction over Luni basin ([in north-western part of](#)  
374 [India](#)). Retrospective TRMM-R maps for low rainfall regime (Fig. 6d) show that the low  
375 rainfall was best captured in high rainfall areas of the Western Ghats, the Indo-Gangetic plain  
376 and the Eastern coastal basins, which is not very surprising as TRMM doesn't detect low  
377 rainfall magnitudes very well, thus suffering from overprediction in arid and semi-arid basins.  
378 Improvement in the low rainfall sensors in IMERG has improved low rainfall estimates, but it  
379 still suffers from gross overprediction in semi-arid areas (as evident in the semi-arid basins in  
380 North-West India (Fig. 6f)).

**Deleted:** near the Western coast of Rajasthan

381 The medium rainfall spatial maps (Figs. 6g–i) suggest similar spatial bias pattern in  
382 TRMM and IMERG. Both TRMM and IMERG suffer from underprediction (negative bias)  
383 in the high elevation Northern basins (of Indus and Jhelum), although IMERG seem to be less  
384 biased than TRMM. Both show similar trends in the Western Ghats, with low bias. However,  
385 both the products show large positive bias (overprediction) in the Middle Godavari basin,  
386 unable to capture the sharp topographic gradient in the region. IMERG slightly overpredicts  
387 rainfall in the North Eastern basins (of Brahmaputra and Barak). The retrospective TRMM  
388 maps for medium rainfall (Fig. 6g) show low bias over entire India, except over the Western  
389 Ghats (slight underprediction) and high elevation Northern basins of Indus and Jhelum  
390 (strong underprediction).

391 The high rainfall spatial maps (Figs. 6j–l) suggest similar spatial pattern in TRMM  
392 and IMERG, with slight negative bias over majority of the basins. The high rainfall in the  
393 Western Ghats is well represented in TRMM and IMERG, however with strong  
394 overprediction in the leeward side of the Western Ghats, suggesting that IMERG is unable to  
395 capture the sharp topographic gradients. IMERG shows greater underprediction in the high  
396 rainfall areas of the North Eastern basins than TRMM, however giving better estimates in the  
397 high elevation basins in Northern India. Both IMERG and TRMM give similar bias pattern in

399 the Indo-Gangetic plain and the semi-arid areas of the North-West. The retrospective  
400 TRMM-R map of high rainfall (Fig. 6j) suggests spatially homogeneous trends throughout  
401 India. However, it suffers from gross underestimation in the high elevation basins of  
402 Northern India (Indus, Jhelum and Chenab). It is clearly observed that the high elevation  
403 basins are an outlier in most of the analysis. A systematic dependence of bias with elevation  
404 may be an underlying trend which is further explored in section 3.5.

### 405 3.4 Threshold statistics

406 Increasing rainfall threshold leads to deteriorating trends in POD and FAR across  
407 majority of the basins, with decreasing POD and increasing FAR. Table 6 summarizes the  
408 number of basins in which IMERG/TRMM gives higher/lower threshold statistics, including  
409 the basins in which they show similar results. At low rainfall threshold, IMERG shows major  
410 improvement in POD in the Western region of Gujarat (Luni, Bhadar and Setrunji basins)  
411 (Figs. 7b,c). The average POD (low rainfall threshold) across basins is 0.95 for IMERG and  
412 0.91 for TRMM. At medium rainfall threshold, average POD across basins is 0.87 for both  
413 IMERG and TRMM. Notably, IMERG gives lower POD (medium rainfall threshold) in two  
414 (Barak and Brahmaputra lower sub-basin) out of the three North-Eastern basins, and higher  
415 POD (medium rainfall threshold) in the semi-arid basins of Rajasthan and Gujarat (Luni,  
416 Bhadar and Setrunji basins) (Figs. 7e,f). At high rainfall threshold, average POD across  
417 basins is 0.76 for IMERG and 0.77 for TRMM. There is notable fall in performance in all the  
418 three North-Western basins. IMERG gives slightly higher POD (high rainfall threshold) in  
419 the high elevation Northern basins (Upper Indus and Jhelum basins) (Figs. 7h,i). At very high  
420 rainfall threshold, average POD across basins is 0.72 for IMERG and 0.7 for TRMM. At very  
421 high rainfall threshold, it's clear that POD of IMERG is worse for all the three North-Eastern  
422 basins and over the semi-arid basins of Rajasthan and Gujarat (Figs. 7k,l). There is slight  
423 improvement in POD values for the high elevation Northern basins (Chenab, Ravi, Beas and  
424 Satulaj basins).

425 At low rainfall threshold, the average FAR across basins is 0.24 for TRMM and 0.22  
426 for IMERG. At medium rainfall threshold, average FAR across basins is 0.22 for TRMM and  
427 0.19 for IMERG. Notably, IMERG outperforms TRMM at low and medium rainfall  
428 thresholds giving lower FAR in the Western basins of Gujarat (Luni and Setrunji basins)  
429 (Figs. 8b,c,e,f). At high rainfall threshold, average FAR across basins is 0.18 for IMERG and  
430 0.22 for TRMM. Slightly reduced FAR are seen in Central India (Yamuna and Chambal

Deleted: i

432 basins) and the North-Eastern basins (Brahmaputra basin) in IMERG at high rainfall  
433 threshold (Figs. 8h,i). At very high rainfall threshold, average FAR across basins is 0.33 for  
434 IMERG and 0.41 for TRMM. There are notably fewer false alarms in IMERG estimates over  
435 the Northern, North-Eastern basins and the Western Ghats at very high thresholds. Both  
436 products give similar FAR (very high threshold) along the Eastern coast and Deccan Plateau  
437 basins.

438 POD for TRMM-R suggests decreasing POD and increasing FAR with increasing  
439 rainfall threshold (Figs. 7a,d,g,j, Figs. 8a,d,g,j). The average POD across basins is 0.89, 0.85,  
440 0.77 and 0.66 for low, medium, high and very high rainfall thresholds, respectively. The  
441 respective FAR values are 0.26, 0.22, 0.21 and 0.43. At high and very high threshold, POD  
442 drops significantly over the high elevation Northern basins and high rainfall North-Eastern  
443 basins and the Western Ghats) (Figs. 7g,j). High FAR is recorded in the [semi-arid](#) basins in  
444 Gujarat [and Rajasthan](#) (Luni and Setrunji) and Central India (Bhadar and Chambal) at low  
445 and medium rainfall threshold (Figs. 8a,d) suggesting TRMM creates a lot of false alarms at  
446 low and medium rainfall magnitudes. There is a sharp contrast between FAR at high and very  
447 high thresholds, with low FAR at high rainfall threshold (75 percentile) and high FAR at very  
448 high threshold (95 percentile) (Figs. 8g,j). This suggests that TRMM-R creates a lot of false  
449 alarms at very high rainfall thresholds, especially in the North-Eastern, Northern and extreme  
450 Southern basins (Fig 8j).

### 451 3.5 Systematic error in satellite estimates as a function of annual rainfall and mean 452 elevation

453 The satellite precipitation estimates were evaluated against a climatologic parameter  
454 (long term annual rainfall of basin) and a topographic parameter (basin mean elevation), to  
455 investigate any systematic variation in errors with climatology or topography. [We found](#) there  
456 is no systematic dependence between the climatologic and topographic parameter ( $R = 0.07$ ,  
457 Fig S3) and they can be considered as independent (implying minimal interference).

458 TRMM-R rainfall estimates exhibited very strong dependence on mean basin  
459 elevation, with decreasing skill (larger bias and lower correlation) in basins with high mean  
460 elevation (Figs. [S4](#), and [S5](#)). For medium and high rainfall regimes (Figs. [S4c](#), d), bias values  
461 were highly negative for high elevation basins (especially for basins with mean elevation >  
462 2000 m), implying underprediction. The corresponding correlation values (Figs. [S5c](#), d) also  
463 suggested reduced skill at high elevation basins.

Deleted: if there was

Deleted: T

Deleted: 9

Deleted: 10

Deleted: 9

Deleted: 10

470 For the year 2014, the systematic dependence of bias on basin elevation improved in  
471 IMERG estimates, with correlation between basin-wise bias and elevation reducing from -  
472 0.43 to -0.32 for medium rainfall intensity (Fig. S6c) and from -0.31 to -0.08 for high rainfall  
473 intensity (Fig. S6d). The same was not observed in the correlation plots (Fig. S7). At low  
474 rainfall intensity (Fig. S7b), IMERG estimates exhibited stronger systematic relationship  
475 between basin-wise correlation and elevation, with strongly decreasing correlation with  
476 elevation than TRMM. At medium rainfall intensity (Fig. S7c), both TRMM and IMERG  
477 showed decreasing skill with increasing elevation. This systematic dependence was stronger  
478 in IMERG than TRMM, as reflected in the higher negative correlation between basin-wise  
479 correlation and elevation in medium rainfall IMERG estimates (Fig. S7c).

480 The same analysis was repeated against mean annual precipitation (Figs. S8-S11)  
481 wherein systematic error dependence was found to be smaller. TRMM-R rainfall estimates  
482 exhibited systematic dependence of bias and correlation with basin wise mean annual rainfall  
483 for low and medium rainfall estimates (Fig. S8 and S9). At low rainfall intensity, TRMM-R  
484 estimates for basins experiencing low annual rainfall were found to be strongly positively  
485 biased (Fig. S8b), implying significant over-estimation. For the year 2014, systematic  
486 dependence of bias was reduced in IMERG at medium rainfall intensities (Fig. S10c,  
487 correlation improved from -0.43 in TRMM to -0.3 for IMERG). A substantial skill was lost in  
488 terms of decreasing correlation for basins receiving high rainfall in both TRMM and IMERG  
489 estimates (Fig. S11c). At high rainfall intensities, bias was more negative (implying  
490 underprediction) in basins which received more rainfall in both IMERG and TRMM (Fig.  
491 S10d).

### 492 3.6 Rainfall-runoff modeling

493 Rainfall-runoff modeling was carried out over Hirakud catchment of Mahanadi River  
494 basin and Wainganga catchment of Godavari River basin, with the calibration and validation  
495 periods as 2000-2011 and 2012-2014, respectively. VIC was first calibrated with IMD  
496 gridded precipitation and then with TRMM3B42 V7. The two calibrated models were then  
497 forced with TRMM and IMERG precipitation for the year 2014 (April – December). Tables 7  
498 and 8 show the model performances.

499 The IMD calibrated model showed better simulations compared to the TRMM  
500 calibrated model, with higher NSE, coefficient of determination and smaller bias and RMSE  
501 in both Wainganga and Hirakud basins. TRMM calibrated model showed overprediction

Deleted: 11

Deleted: 11

Deleted: 12

Deleted: 12

Deleted: 12

Deleted: 12

Deleted: 4

Deleted: 7

Deleted: 4

Deleted: 5

Deleted: 4

Deleted: 6

Deleted: 7

Deleted: 6

516 (positive bias) in Hirakud basin, but was relatively unbiased in Wainganga basin ( $-10 \leq$   
517  $P_{bias} \leq 10$ ) (Tables 7, 8).

518 The IMERG simulations with IMD and TRMM calibrated models were slightly  
519 inferior in comparison with TRMM simulations for 2014 (NSE = 0.64 for IMERG and 0.72  
520 for TRMM in IMD calibration; NSE = 0.7 for IMERG and 0.72 for TRMM in TRMM  
521 calibration) (Table 7, Fig. 9) for Hirakud. However, the IMERG simulations gave similar  
522 results as TRMM in Wainganga basin when calibrated using IMD data, but inferior results  
523 when calibrated with TRMM data (NSE = 0.61 for IMERG and 0.72 for TRMM) (Table 8,  
524 Fig. 10). In case of Hirakud basin, IMERG simulations gave higher NSE when calibrated  
525 with TRMM data. However, in the case of Wainganga basin, IMERG gave higher NSE when  
526 calibrated with IMD data. The high negative bias in IMERG simulations (with IMD and  
527 TRMM calibrated models) showed significant underprediction compared to TRMM.

528 Both TRMM and IMERG underestimated the magnitude of the two major peaks (flow  
529  $> 15000 \text{ m}^3/\text{s}$ ) in Hirakud and Wainganga basin in 2014 (Figs. 9, 10). However, the phase  
530 was well captured by both IMERG and TRMM in the two basins. IMERG overestimated low  
531 flows for the majority of time in both IMD and TRMM calibrated VIC model for both the  
532 basins, and thus was inferior in performance to TRMM. This suggests that the use of an  
533 appropriate post-processor for streamflow (Ye et al., 2014) could tremendously benefit the  
534 flow simulations, which might be an interesting study for the future.

#### 535 4 Conclusions

536 TRMM 3B42 and IMERG precipitation estimates were comprehensively evaluated over  
537 86 basins in India. TRMM 3B42 was analysed for two distinct time periods, the retrospective  
538 analysis was carried out from 1998-2013 and the current estimates were compared with  
539 IMERG for the year 2014 (March 12<sup>th</sup> 2014 – December 31<sup>st</sup> 2014). The systematic biases in  
540 both the estimates were explored with respect to a climatologic parameter (basin mean annual  
541 rainfall) and a topographic parameter (basin mean elevation). Finally, TRMM and IMERG  
542 were hydrologically evaluated by carrying out rainfall-runoff modeling over Hirakud  
543 catchment of Mahanadi River basin and Wainganga catchment of Godavari River basin. The  
544 results of the study are summarized as:

- 545 1. IMERG rainfall estimates were found to be better than TRMM at all rainfall intensities, in  
546 terms of correlation. IMERG outperformed TRMM in 60, 52, 52 and 55 out of 86 basins

Deleted: 13

Deleted: 4

Deleted: over

Deleted: 13

Deleted: 4

Deleted: (in form of real-time error updation)



553 for overall, low, medium and high rainfall regimes.

554 2. IMERG gave better estimates of low rainfall magnitudes with smaller biases in 75 out of  
555 the 86 basins analysed, which suggests that the sensor improvement in IMERG satellite  
556 translated into better low rainfall estimation. IMERG captured the low rainfall  
557 magnitudes better over the Indo-Gangetic plain, North-Eastern basins of Brahmaputra and  
558 Barak, Central India (Mahi and the Indo-Gangetic plain) and the rain shadow area of the  
559 Western Ghats. However, for the semi-arid North Western basins, TRMM low rainfall  
560 estimates outperformed IMERG.

561 3. The high rainfall estimates of IMERG outperformed TRMM in the rain-shadow area of  
562 the Western Ghats, the high elevation basins of the North and the South-Eastern basins of  
563 Pennar and Cauvery. However, TRMM did a better job in the North-Eastern basins of  
564 Brahmaputra and Barak and the North-Western basins of Rajasthan.

565 4. Increasing rainfall thresholds lead to deteriorating trends in POD and FAR across  
566 majority of basins, with decreasing POD and increasing FAR. [At very high rainfall](#)  
567 [thresholds \(>95 percentile\), TRMM exhibited high false alarm ratio \(FAR\), especially in](#)  
568 [the North-eastern and Southern basins, implying that they do not capture the extreme](#)  
569 [precipitation magnitudes well. This was also seen in the rainfall-runoff exercise where the](#)  
570 [peak flows were underpredicted in Mahanadi and Wainganga River basins, both in the](#)  
571 [case of TRMM and IMERG.](#)

572 5. The skill of TRMM-R medium rainfall estimates (in terms of Pbias and correlation) was  
573 found to exhibit strong systematic dependence on annual rainfall (climatologic  
574 parameter), with larger bias and lower correlation in basins which received higher annual  
575 rainfall. This systematic dependence was reduced significantly in IMERG estimates.  
576 However, no such improvement was found at low and high rainfall intensities.

577 6. A very strong deteriorating skill (increasing bias and decreasing correlation) was found in  
578 TRMM-R rainfall estimates at all intensities in the high elevation basins. This systematic  
579 dependence was strongly reduced in IMERG estimates at all rainfall intensities,  
580 suggesting IMERG captures the rainfall trends better with respect to topography.

581 7. Rainfall runoff modeling using VIC model over Mahanadi and Wainganga River basins  
582 gave better results with TRMM as input forcing, rather than IMERG. Both TRMM and  
583 IMERG captured the phase of the peak flows, however both underreported the  
584 magnitudes. Low flows were grossly over predicted by IMERG, which led to overall poor  
585 performance with IMERG. As GPM is still a young mission, with time a longer  
586 timeseries of IMERG will help in model evaluation as IMERG can be used to directly

Deleted:

Deleted: ,

Deleted: Chambal

590 calibrate the model, hence capturing the fine details in the product. [It will also be useful](#)  
591 [to see if other hydrologic models can capture peak flows more accurately when forced](#)  
592 [with TRMM/IMERG in Mahanadi and Wainganga basins. This would mean that the poor](#)  
593 [representation of peak flows is a function of model structural uncertainty, and not the](#)  
594 [satellite precipitation products driving the model. This will make a very interesting future](#)  
595 [case study.](#)

596 In essence, IMERG gives reasonable improvement in rainfall estimates across majority of  
597 the Indian basins. The most notable improvement in IMERG is the reduction in systematic  
598 error dependence on topography (basin mean elevation), which suggests improvements in the  
599 assimilation of satellite observations. The improved sensitivity of Ku and Ka bands in GPM  
600 satellite resulted in improvement in detection of low rainfall magnitudes. The expected  
601 improvement in IMERG in snow detection could not be verified in this study as India is  
602 mostly a tropical country which receives very [scanty snowfall](#). The constant overestimation  
603 of low flow magnitudes in the rainfall-runoff exercise suggest that IMERG may benefit from  
604 a post forecast data assimilation scheme [\(or postprocessing\)](#) (Ye et al., 2014), which is a  
605 worthy topic for further research.

Deleted: less snow

607       **References**

- 608 Akhtar, M. K., Corzo, G. A., van Andel, S. J. and Jonoski, A.: River flow forecasting with  
609 artificial neural networks using satellite observed precipitation pre-processed with flow  
610 length and travel time information: case study of the Ganges river basin, *Hydrol. Earth Syst.*  
611 *Sci.*, 13(9), 1607–1618, doi:10.5194/hess-13-1607-2009, 2009.
- 612 Artan, G., Gadain, H., Smith, J. L., Asante, K., Bandaragoda, C. J. and Verdin, J. P.:  
613 Adequacy of satellite derived rainfall data for stream flow modeling, *Nat. Hazards*, 43, 167–  
614 185, doi:10.1007/s11069-007-9121-6, 2007.
- 615 Bajracharya, S. R., Shrestha, M. S. and Shrestha, A. B.: Assessment of high-resolution  
616 satellite rainfall estimation products in a streamflow model for flood prediction in the  
617 Bagmati basin, Nepal, *J. Flood Risk Manag.*, 1–12, doi:10.1111/jfr3.12133, 2014.
- 618 Bisht, D. S., Chatterjee, C., Raghuvanshi, N. S. and Sridhar, V.: Spatio-temporal trends of  
619 rainfall across Indian river basins, *Theor. Appl. Climatol.*, 1–18, doi:10.1007/s00704-017-  
620 2095-8, 2017.
- 621 Collischonn, B., Collischonn, W. and Tucci, C. E. M.: Daily hydrological modeling in the  
622 Amazon basin using TRMM rainfall estimates, *J. Hydrol.*, 360, 207–216,  
623 doi:10.1016/j.jhydrol.2008.07.032, 2008.
- 624 Duband, D., Obled, C. and Rodriguez, J. Y.: Unit hydrograph revisited: an alternate iterative  
625 approach to UH and effective precipitation identification, *J. Hydrol.*, 150(1), 115–149,  
626 doi:10.1016/0022-1694(93)90158-6, 1993.
- 627 Gao, Y. C. and Liu, M. F.: Evaluation of high-resolution satellite precipitation products using  
628 rain gauge observations over the Tibetan Plateau, *Hydrol. Earth Syst. Sci.*, 17(2), 837–849,  
629 doi:10.5194/hess-17-837-2013, 2013.
- 630 Hamlet, A. F. and Lettenmaier, D. P.: Columbia River Streamflow Forecasting Based on  
631 ENSO and PDO Climate Signals, *J. Water Resour. Plan. Manag.*, 125(6), 333–341,  
632 doi:10.1061/(ASCE)0733-9496(1999)125:6(333), 1999.
- 633 Hou, A. Y., Kakar, R. K., Neeck, S., Azarbarzin, A. A., Kummerow, C. D., Kojima, M., Oki,  
634 R., Nakamura, K. and Iguchi, T.: The Global Precipitation Measurement Mission, *Bull. Am.*  
635 *Meteorol. Soc.*, 95(5), 701–722, doi:10.1175/BAMS-D-13-00164.1, 2014.

636 Huffman, G. J., Bolvin, D. T., Nelkin, E. J., Wolff, D. B., Adler, R. F., Gu, G., Hong, Y.,  
637 Bowman, K. P. and Stocker, E. F.: The TRMM Multisatellite Precipitation Analysis (TMPA):  
638 Quasi-Global, Multiyear, Combined-Sensor Precipitation Estimates at Fine Scales, *J.*  
639 *Hydrometeorol.*, 8(1), 38–55, doi:10.1175/JHM560.1, 2007.

640 Huffman, G. J., Bolvin, D. T. and Nelkin, E. J.: Integrated Multi-satellite Retrievals for GPM  
641 (IMERG) Technical Documentation, 2014.

642 India, G. of: Watershed Atlas of India. [online] Available from: [http://india-](http://india-wris.nrsc.gov.in/Publications/WatershedSubbasinAtlas/Watershed Atlas of India.pdf)  
643 [wris.nrsc.gov.in/Publications/WatershedSubbasinAtlas/Watershed Atlas of India.pdf](http://india-wris.nrsc.gov.in/Publications/WatershedSubbasinAtlas/Watershed Atlas of India.pdf), 2014.

644 Jena, P. P., Chatterjee, C., Pradhan, G. and Mishra, A.: Are recent frequent high floods in  
645 Mahanadi basin in eastern India due to increase in extreme rainfalls?, *J. Hydrol.*, 517, 847–  
646 862, doi:10.1016/j.jhydrol.2014.06.021, 2014.

647 Kneis, D., Chatterjee, C. and Singh, R.: Evaluation of TRMM rainfall estimates over a large  
648 Indian river basin (Mahanadi), *Hydrol. Earth Syst. Sci.*, 18(7), 2493–2502 [online] Available  
649 from: <http://www.hydrol-earth-syst-sci-discuss.net/11/1169/2014/hessd-11-1169-2014.pdf>  
650 (Accessed 20 October 2014), 2014.

651 Liang, X., Lettenmaier, D. P., Wood, E. F. and Burges, S. J.: A simple hydrologically based  
652 model of land surface water and energy fluxes for general circulation models, *J. Geophys.*  
653 *Res.*, 99(D7), 14415, doi:10.1029/94JD00483, 1994.

654 Liang, X., Wood, E. F. and Lettenmaier, D. P.: Surface soil moisture parameterization of the  
655 VIC-2L model: Evaluation and modification, *Glob. Planet. Change*, 13, 195–206,  
656 doi:10.1016/0921-8181(95)00046-1, 1996.

657 Liu, Z.: Comparison of Integrated Multi-satellite Retrievals for GPM (IMERG) and TRMM  
658 Multi-satellite Precipitation Analysis (TMPA) Monthly Precipitation Products: Initial  
659 Results, *J. Hydrometeorol.*, 17, 777–790, doi:10.1175/JHM-D-15-0068.1, 2016.

660 Lohmann, D., Nolte-Holube, R. and Raschke, E.: A large-scale horizontal routing model to  
661 be coupled to land surface parametrization schemes, *Tellus A*, 48(5), 708–721,  
662 doi:10.1034/j.1600-0870.1996.t01-3-00009.x, 1996.

663 McCuen, R. H.: Assessment of Hydrological and Statistical Significance, *J. Hydrol. Eng.*,  
664 21(4), 2516001, doi:10.1061/(ASCE)HE.1943-5584.0001340, 2016.

665 Melsen, L. A., Teuling, A. J., Torfs, P. J. J. F., Uijlenhoet, R., Mizukami, N. and Clark, M.  
666 P.: HESS Opinions: The need for process-based evaluation of large-domain hyper-resolution  
667 models, *Hydrol. Earth Syst. Sci.*, 20(3), 1069–1079, doi:10.5194/hess-20-1069-2016, 2016.

668 Mujumdar, P. P.: Share data on water resources, *Nature*, 521(7551), 151–152, 2015.

669 Pai, D. S., Sridhar, L., Rajeevan, M., Sreejith, O. P., Satbhai, N. S. and Mukhopadhyay, B.:  
670 Development of a new high spatial resolution (0.25× 0.25) long period (1901–2010) daily  
671 gridded rainfall data set over India and its comparison with existing data sets over the region.,  
672 *Mausam*, 65(1), 1–18, 2014.

673 Peng, B., Shi, J., Ni-Meister, W., Zhao, T. and Ji, D.: Evaluation of TRMM Multisatellite  
674 Precipitation Analysis (TMPA) Products and Their Potential Hydrological Application at an  
675 Arid and Semiarid Basin in China, *IEEE J. Sel. Top. Appl. Earth Obs. Remote Sens.*, 7(9),  
676 3915–3930, doi:10.1109/JSTARS.2014.2320756, 2014.

677 Prakash, S., Mitra, A. K., Momin, I. M., Gairola, R. M., Pai, D. S., Rajagopal, E. N. and  
678 Basu, S.: A review of recent evaluations of TRMM Multisatellite Precipitation Analysis  
679 (TMPA) research products against ground-based observations over Indian land and oceanic  
680 regions, *MAUSAM*, 66(3), 355–366 [online] Available from:  
681 [https://www.researchgate.net/profile/Satya\\_Prakash/publication/281115874\\_A\\_review\\_of\\_re](https://www.researchgate.net/profile/Satya_Prakash/publication/281115874_A_review_of_recent_evaluations_of_TRMM_Multisatellite_Precipitation_Analysis_(TMPA)_research_products_against_ground-based_observations_over_Indian_land_and_oceanic_regions/links/55e)  
682 [cent\\_evaluations\\_of\\_TRMM\\_Multisatellite\\_Precipitation\\_Analysis\\_\(TMPA\)\\_research\\_pro](https://www.researchgate.net/profile/Satya_Prakash/publication/281115874_A_review_of_recent_evaluations_of_TRMM_Multisatellite_Precipitation_Analysis_(TMPA)_research_products_against_ground-based_observations_over_Indian_land_and_oceanic_regions/links/55e)  
683 [ducts\\_against\\_ground-based\\_observations\\_over\\_Indian\\_land\\_and\\_oceanic\\_regions/links/55e](https://www.researchgate.net/profile/Satya_Prakash/publication/281115874_A_review_of_recent_evaluations_of_TRMM_Multisatellite_Precipitation_Analysis_(TMPA)_research_products_against_ground-based_observations_over_Indian_land_and_oceanic_regions/links/55e),  
684 2015.

685 Prakash, S., Mitra, A. K., AghaKouchak, A., Liu, Z., Norouzi, H. and Pai, D. S.: A  
686 preliminary assessment of GPM-based multi-satellite precipitation estimates over a monsoon  
687 dominated region, *J. Hydrol.*, doi:10.1016/j.jhydrol.2016.01.029, 2016a.

688 Prakash, S., Mitra, A. K., Pai, D. S. and AghaKouchak, A.: From TRMM to GPM: How well  
689 can heavy rainfall be detected from space?, *Adv. Water Resour.*, 88, 1–7,  
690 doi:10.1016/j.advwatres.2015.11.008, 2016b.

691 Schumann, A. H.: Thiessen Polygon Thiessen polygon BT - Encyclopedia of  
692 Hydrology and Lakes, pp. 648–649, Springer Netherlands, Dordrecht , 1998.

693 Shah, H. L. and Mishra, V.: Uncertainty and Bias in Satellite-based Precipitation Estimates  
694 over Indian Sub-continental Basins: Implications for Real-time Streamflow Simulation and

695 Flood Prediction, *J. Hydrometeorol.*, 17(2), 615–636, doi:10.1175/JHM-D-15-0115.1, 2016.

696 Srivastava, A. K., Rajeevan, M. and Kshirsagar, S. R.: Development of a high resolution  
697 daily gridded temperature data set (1969-2005) for the Indian region, *Atmos. Sci. Lett.*, 10(4),  
698 249–254, doi:10.1002/asl.232, 2009.

699 Tang, G., Ma, Y., Long, D., Zhong, L. and Hong, Y.: Evaluation of GPM Day-1 IMERG and  
700 TMPA Version-7 legacy products over Mainland China at multiple spatiotemporal scales, *J.*  
701 *Hydrol.*, 533, 152–167, doi:10.1016/j.jhydrol.2015.12.008, 2016a.

702 Tang, G., Zeng, Z., Long, D., Guo, X., Yong, B., Zhang, W. and Hong, Y.: Statistical and  
703 Hydrological Comparisons between TRMM and GPM Level-3 Products over a Midlatitude  
704 Basin: Is Day-1 IMERG a Good Successor for TMPA 3B42V7?, *J. Hydrometeorol.*, 17(1),  
705 121–137, doi:10.1175/JHM-D-15-0059.1, 2016b.

706 Tawde, S. A. and Singh, C.: Investigation of orographic features influencing spatial  
707 distribution of rainfall over the Western Ghats of India using satellite data, *Int. J. Climatol.*,  
708 35(9), 2280–2293, doi:10.1002/joc.4146, 2015.

709 Tong, K., Su, F., Yang, D. and Hao, Z.: Evaluation of satellite precipitation retrievals and  
710 their potential utilities in hydrologic modeling over the Tibetan Plateau, *J. Hydrol.*, 519, 423–  
711 437, doi:10.1016/j.jhydrol.2014.07.044, 2014.

712 Wu, H., Adler, R. F., Hong, Y., Tian, Y. and Policelli, F.: Evaluation of Global Flood  
713 Detection Using Satellite-Based Rainfall and a Hydrologic Model, *J. Hydrometeorol.*, 13(4),  
714 1268–1284, doi:10.1175/JHM-D-11-087.1, 2012.

715 Wu, X., Xiang, X., Li, L. and Wang, C.: Water level updating model for flow calculation of  
716 river networks, *Water Sci. Eng.*, 7(1), 60–69, doi:10.3882/j.issn.1674-2370.2014.01.007,  
717 2014.

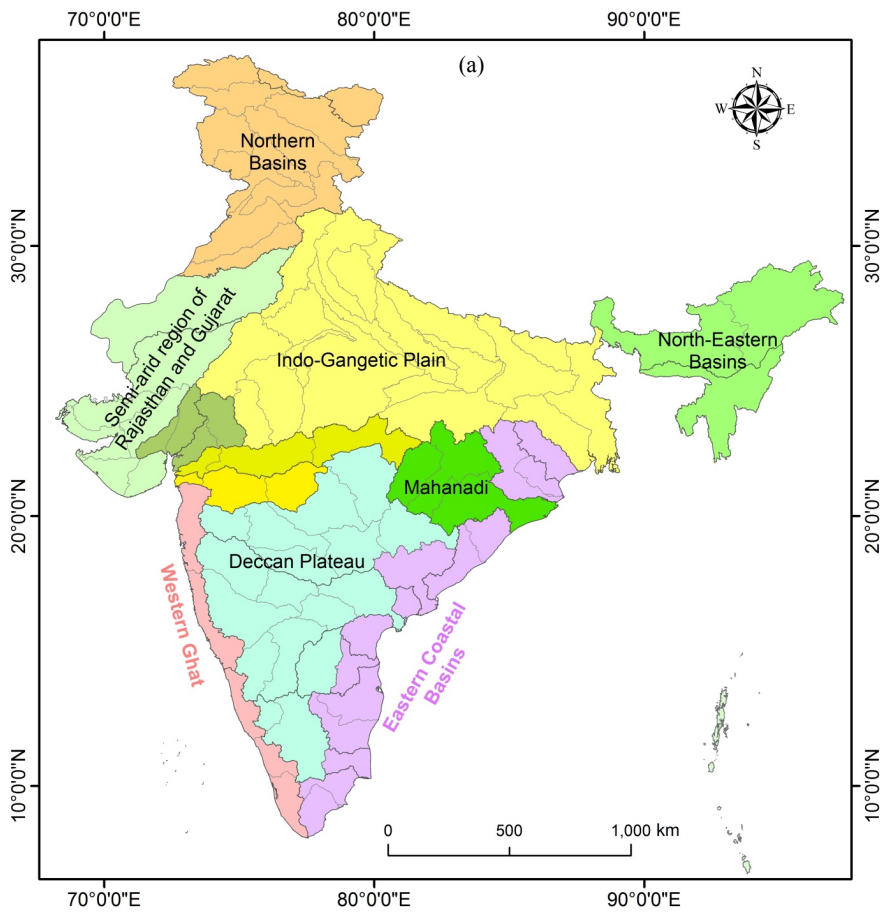
718 Ye, A., Duan, Q., Yuan, X., Wood, E. F. and Schaake, J.: Hydrologic post-processing of  
719 MOPEX streamflow simulations, *J. Hydrol.*, 508(Supplement C), 147–156,  
720 doi:https://doi.org/10.1016/j.jhydrol.2013.10.055, 2014.

721 Yong, B., Hong, Y., Ren, L.-L., Gourley, J. J., Huffman, G. J., Chen, X., Wang, W. and  
722 Khan, S. I.: Assessment of evolving TRMM-based multisatellite real-time precipitation  
723 estimation methods and their impacts on hydrologic prediction in a high latitude basin, *J.*

724 Geophys. Res., 117(D9), doi:10.1029/2011JD017069, 2012.

725 Zhu, Q., Xuan, W., Liu, L. and Xu, Y.: Evaluation and hydrological application of  
726 precipitation estimates derived from PERSIANN CDR, TRMM 3B42V7 and NCEP CFSR  
727 over humid regions in China, Hydrol. Process., 30(17), 3061–3083, doi:10.1002/hyp.10846,  
728 2016.

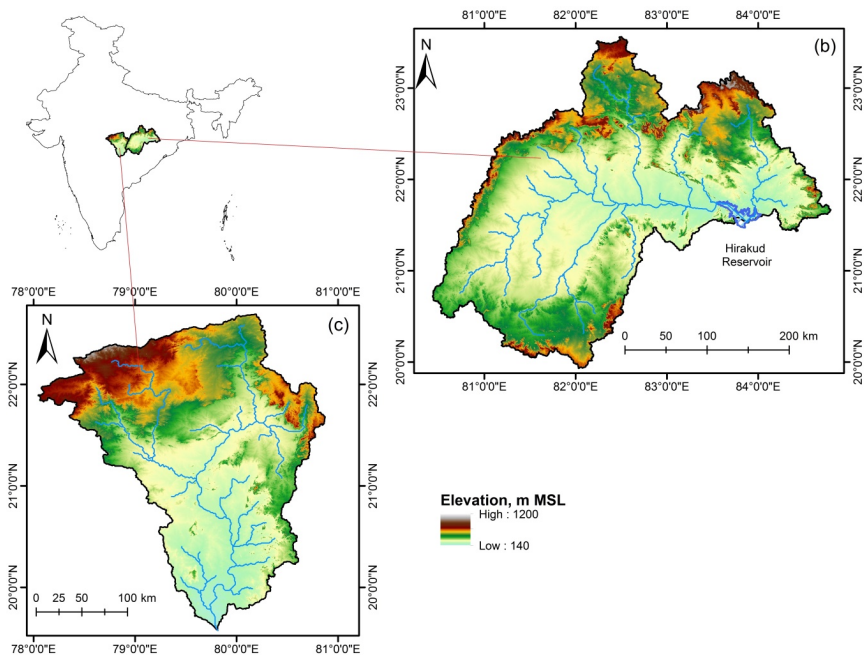
729



730

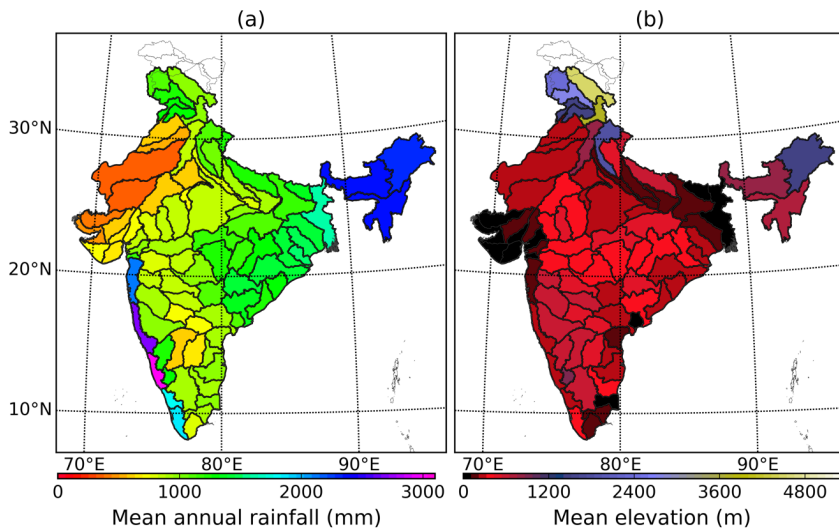
731

732



733  
 734 **Figure 1(a).** Map of the major basins in India including west and east flowing rivers, map of  
 735 (b) Hirkud catchment of the Mahanadi River basin and (c) Wainganga catchment of the  
 736 Godavari River basin.





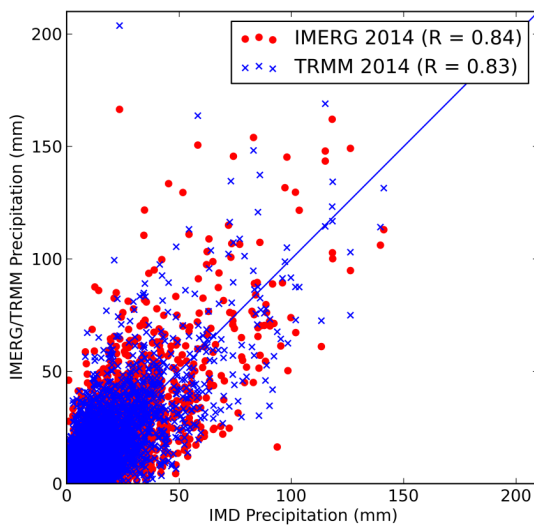
737

738 **Figure 2.** Spatial distribution of (a) long term average annual rainfall (calculated from IMD  
 739 gridded rainfall dataset during 1980-2010), and (b) average elevation above mean sea level  
 740 (calculated using SRTM DEM) over 86 delineated river basins across India.

Deleted: from years

Deleted: major

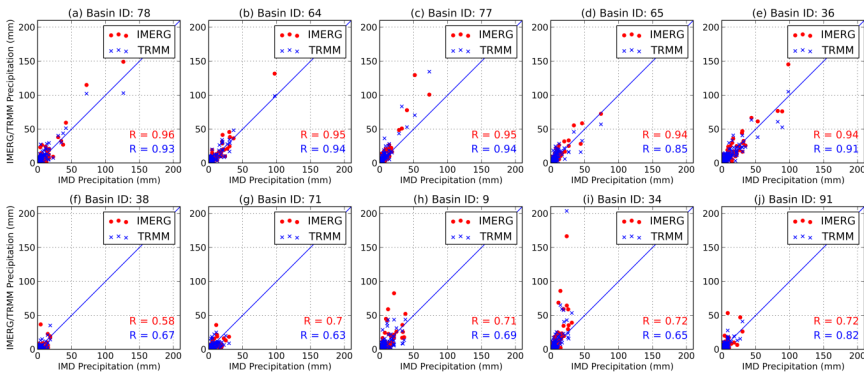
Deleted: in



741

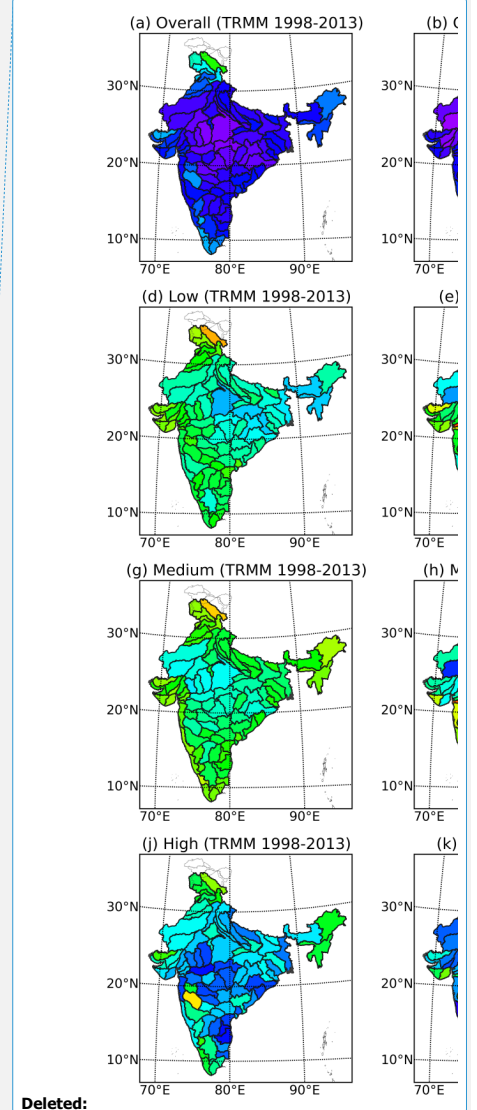
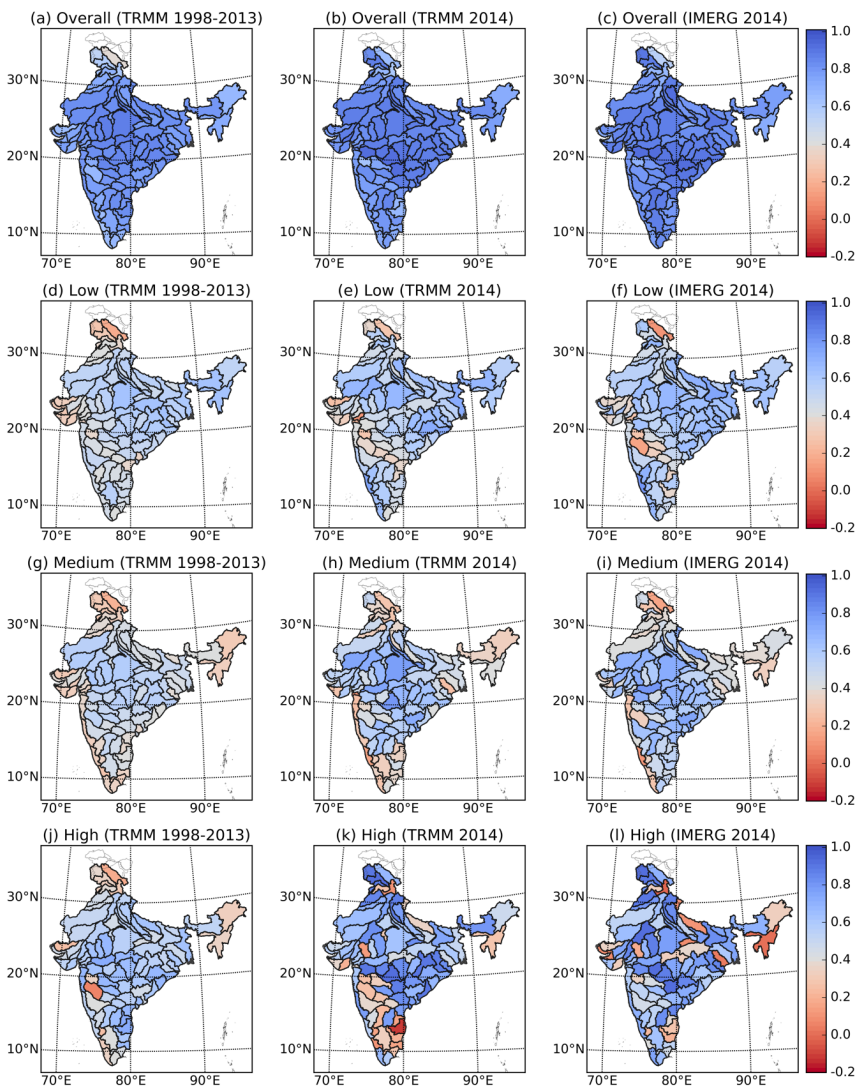
745 **Figure 3.** Scatterplot of satellite precipitation products (TRMM and IMERG) vs observed  
 746 rainfall (IMD) computed over 86 delineated river basins across India (based on daily  
 747 precipitation data from March 12, 2014 to December 31, 2014).

Deleted: major  
 Deleted: in



748

749 **Figure 4.** Scatterplot of satellite precipitation products (TRMM and IMERG) vs observed  
 750 rainfall (IMD) for (a) – (e) five best basins in terms of correlation of IMERG with IMD  
 751 (arranged in descending order) and (f) – (j) five worse basins in terms of correlation of  
 752 IMERG with IMD (arranged in ascending order) (based on daily precipitation data from  
 753 March 12, 2014 to December 31, 2014).



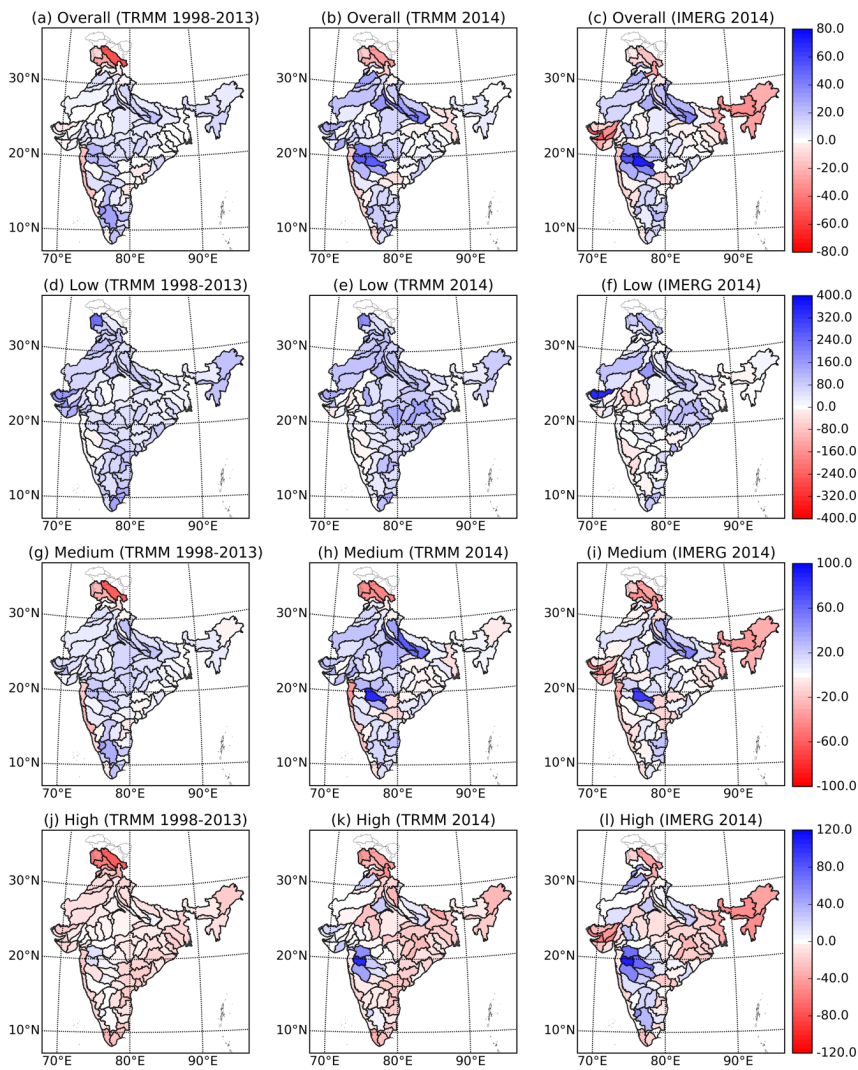
Deleted:

Deleted: major

Deleted: in

756

757 **Figure 5.** Spatial representation of correlation of TRMM (1998-2013), TRMM (2014) and  
 758 IMERG (2014) over 86 delineated river basins across India for (a) – (c) overall time series,  
 759 (d) – (f) low, (g) – (i) medium and (j) – (l) high rainfall regime.

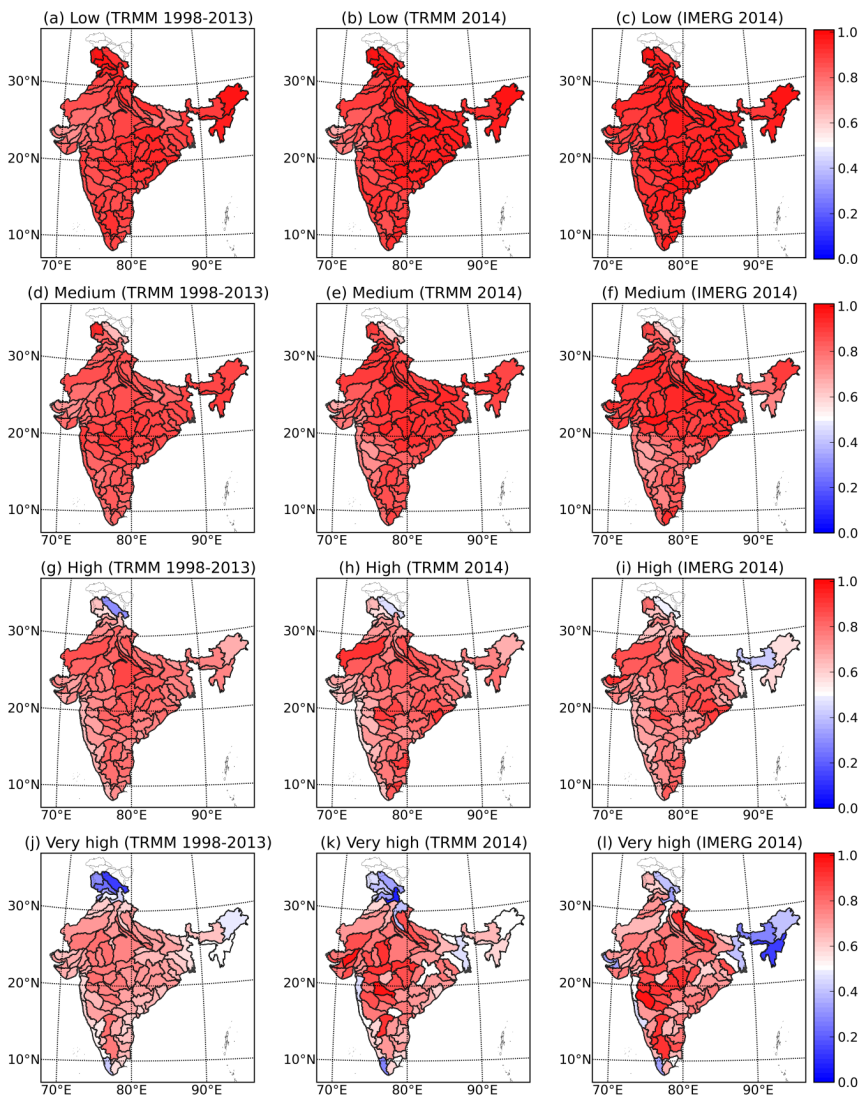


763

764 **Figure 6.** Spatial representation of percentage bias of TRMM (1998-2013), TRMM (2014)  
 765 and IMERG (2014) over 86 delineated river basins across India for (a) – (c) overall time  
 766 series and over (d) – (f) low, (g) – (i) medium and (j) – (l) high rainfall regime.

Deleted: major

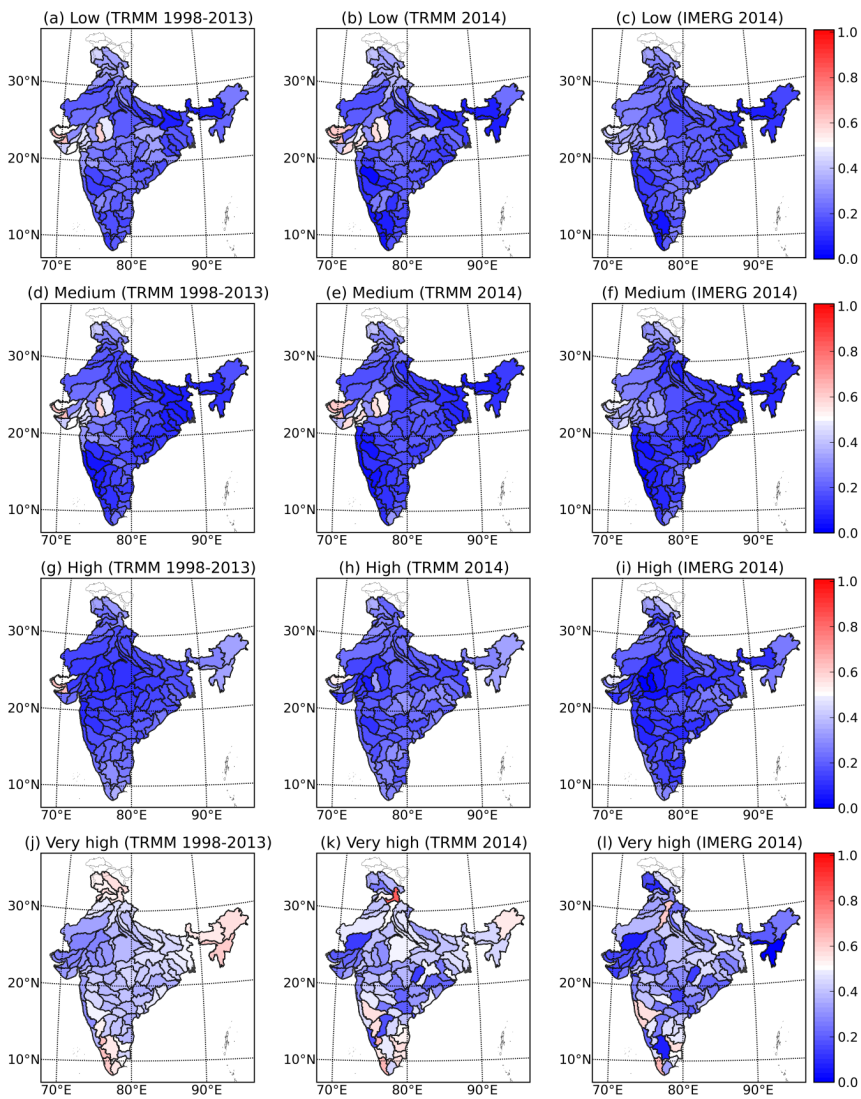
Deleted: in



769

770 **Figure 7.** Spatial representation of probability of detection (POD) for (a) – (c) low (25  
 771 percentile), (d) – (f) medium (50 percentile), (g) – (i) high (75 percentile) and (j) – (l) very  
 772 high (95 percentile) rainfall threshold for TRMM (1998-2013), TRMM (2014) and IMERG  
 773 (2014) rainfall estimates over 86 delineated river basins across India.

Deleted: major  
 Deleted: in

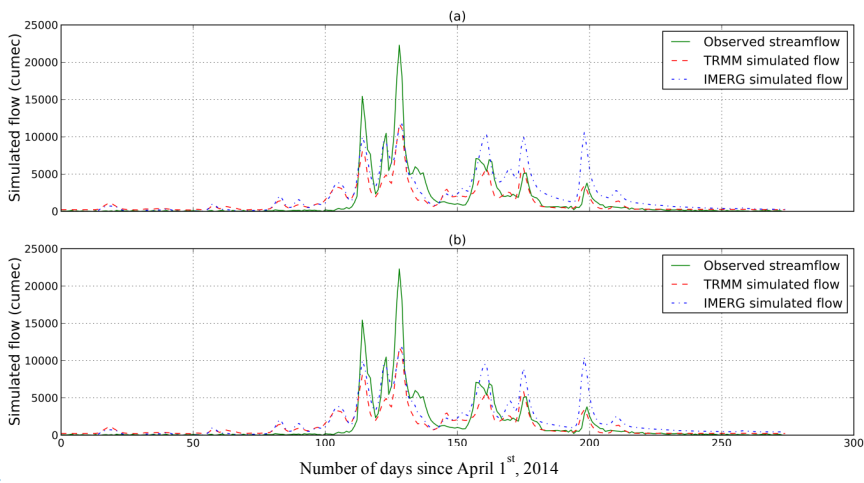


776

777 **Figure 8.** Spatial representation of false alarm ratio (FAR) for (a) – (c) low (25 percentile),  
 778 (d) – (f) medium (50 percentile), (g) – (i) high (75 percentile) and (j) – (l) very high (95  
 779 percentile) rainfall threshold for TRMM (1998-2013), TRMM (2014) and IMERG (2014)  
 780 rainfall estimates over 86 delineated river basins across India.

Deleted: major  
 Deleted: in





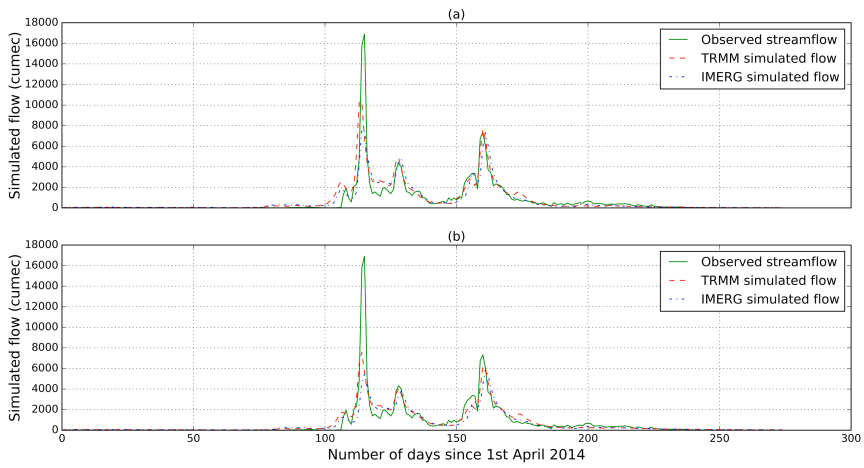
783

784 **Figure 9.** Hydrographs for TRMM and IMERG simulations (April 1, 2014 – December 31,

785 2014) with (a) IMD and (b) TRMM calibrated VIC model for Hirakud basin.

Deleted: ... [1]

Deleted: 13



786

787 **Figure 10.** Hydrographs for TRMM and IMERG simulations (April 1, 2014 – December 31,

788 2014) with (a) IMD and (b) TRMM calibrated VIC model for Wainganga basin.

Deleted: 4

793 **Table 1.** Summary of the precipitation datasets used.

Product name	Spatial resolution	Temporal resolution	Spatial coverage	Temporal coverage	Period used in this study
IMD Gridded Rainfall	0.25° x 0.25°	Daily	Indian landmass	1901-2014	1998-2013, 12 <sup>th</sup> March, 2014 – 31 <sup>st</sup> December 2014
TRMM Research product	0.25° x 0.25°	3-hourly	50° N-S	1998-present	1998-2013, 12 <sup>th</sup> March, 2014 – 31 <sup>st</sup> December 2014
IMERG Final Run	0.1° x 0.1°	Half-hourly	60° N-S	12 <sup>th</sup> March, 2014 - present	12 <sup>th</sup> March, 2014 – 31 <sup>st</sup> December 2014

794 **Table 2.** Contingency table used to calculate probability of detection (POD) and false alarm  
795 ratio (FAR) at a given rainfall threshold.

		Simulated	
		> Threshold	<= Threshold
Observed	> Threshold	HIT	MISS
	<= Threshold	FALSE	NEGATIVE

796 **Table 3.** Summary of different statistical indices used to evaluate the satellite precipitation  
797 products.

Index	Formula	Best value	Worst value
Pearson correlation (R)	$\frac{\sum(X - \bar{X})(Y - \bar{Y})}{\sqrt{\sum(X - \bar{X})^2} \sqrt{\sum(Y - \bar{Y})^2}}$	1	0
Percentage bias (Pbias)	$\frac{\sum(Y - X)}{\sum X} * 100$	0	$+\infty / -\infty$
Probability of detection (POD)	$\frac{HIT}{HIT + MISS}$	1	0
False alarm ratio (FAR)	$\frac{FALSE}{HIT + FALSE}$	0	1
Nash Sutcliffe efficiency (NSE)	$1 - \frac{\sum(X - Y)^2}{\sum(X - \bar{X})^2}$	1	$-\infty$ (negative value means that mean is a better estimator)



			than the model).
Root mean square error (RMSE)	$\sqrt{\frac{\sum(X-Y)^2}{n}}$	0	$+\infty$

Deleted: d

798 ( $X = \text{Observed}$ ,  $\bar{X} = \text{Observed mean}$ ,  $Y = \text{Simulated}$ ,  $\bar{Y} = \text{Simulated mean}$ ,  $n =$   
799  $\text{Data points}$ )

800 **Table 4.** Segregation of overall rainfall time series into low, medium and high rainfall time  
801 series ( $R = \text{Rainfall}$ ,  $\mu = \text{Mean of rainfall}$ ,  $\sigma = \text{Standard deviation of rainfall}$ ).

Rainfall regime	Criterion
Low	$R < \mu$
Medium	$R \geq \mu$ and $R \leq \mu + 2\sigma$
High	$R > \mu + 2\sigma$

802 **Table 5.** Comparison of the IMERG and TRMM based on the number of basins in which the satellite  
803 products show higher/lower correlation based on the year 2014 ( $R$ : Pearson correlation coefficient)

Deleted: p

Expression	IMERG	TRMM
$R > 0.8$	73	68
$R > 0.9$	20	13
Higher R	60	26
Higher R (low rainfall regime)	52	34
Higher R (medium rainfall regime)	52	34
Higher R (high rainfall regime)	55	31

804 **Table 6.** Comparison of the IMERG and TRMM based on the number of basins in which the satellite  
805 products show higher/lower POD/FAR based on the year 2014. The third column gives the number  
806 of basins in which IMERG/TRMM gives similar POD/FAR. (Low, medium, high and very high  
807 threshold: 25, 50, 75, 95 percentile respectively)

Expression	IMERG	TRMM	Similar
Higher POD (low rainfall threshold)	62	24	0
Higher POD (medium rainfall threshold)	39	37	10
Higher POD (high rainfall threshold)	32	45	9
Higher POD (very high rainfall threshold)	44	27	15
Lower FAR (low rainfall threshold)	42	40	4
Lower FAR (medium rainfall threshold)	53	26	7
Lower FAR (high rainfall threshold)	67	15	4
Lower FAR (very high rainfall threshold)	64	17	5

808

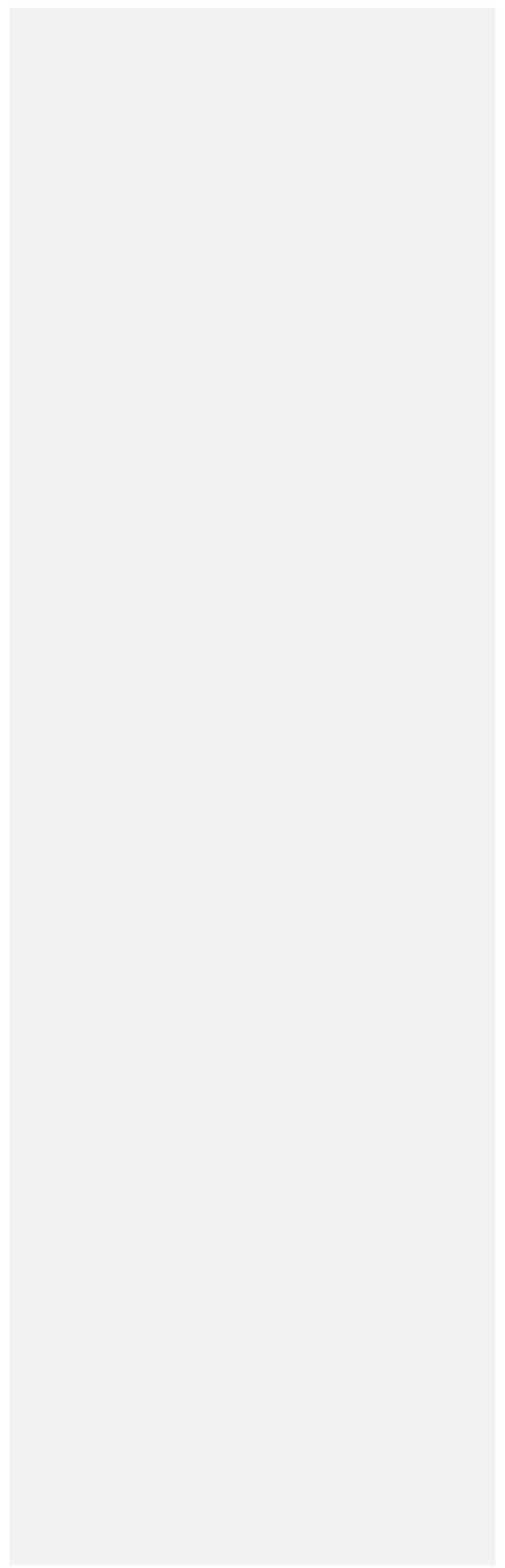
809

812 **Table 7.** Performance statistics for rainfall-runoff modeling using VIC for Hirakud catchment  
 813 of Mahanadi River basin.

	<b>Time period</b>	<b>NSE</b>	<b>R<sup>2</sup></b>	<b>P-bias</b>	<b>RMSE (m<sup>3</sup>/s)</b>
IMD calibration	2000-2011	0.83	0.84	16.78	919.88
IMD validation	2012-2014	0.86	0.88	3.91	823.58
TRMM calibration	2000-2011	0.72	0.74	18.2	1160.94
TRMM validation	2012-2014	0.73	0.74	14	1128.15
TRMM (IMD calibration)	2014	0.72	0.82	-9.41	1591.09
IMERG (IMD calibration)	2014	0.64	0.68	41.4	1786.22
TRMM (TRMM calibration)	2014	0.72	0.82	-9.24	1588.86
IMERG (TRMM calibration)	2014	0.7	0.72	31.32	1641.82

814 **Table 8.** Performance statistics for rainfall-runoff modeling using VIC for Wainganga River  
 815 basin.

	<b>Time period</b>	<b>NSE</b>	<b>R<sup>2</sup> (p-value)</b>	<b>P-bias</b>	<b>RMSE (m<sup>3</sup>/s)</b>
IMD calibration	2000-2011	0.81	0.81	9.18	740.49
IMD validation	2012-2014	0.87	0.88	-10.8	852.9
TRMM calibration	2000-2011	0.7	0.71	15.66	931.65
TRMM validation	2012-2014	0.83	0.83	5.93	973.41
TRMM (IMD calibration)	2014	0.74	0.74	8.70	883.19
IMERG (IMD calibration)	2014	0.74	0.76	-0.52	883.59
TRMM (TRMM calibration)	2014	0.72	0.75	-2.70	922.04
IMERG (TRMM calibration)	2014	0.61	0.66	-12.10	1082.34



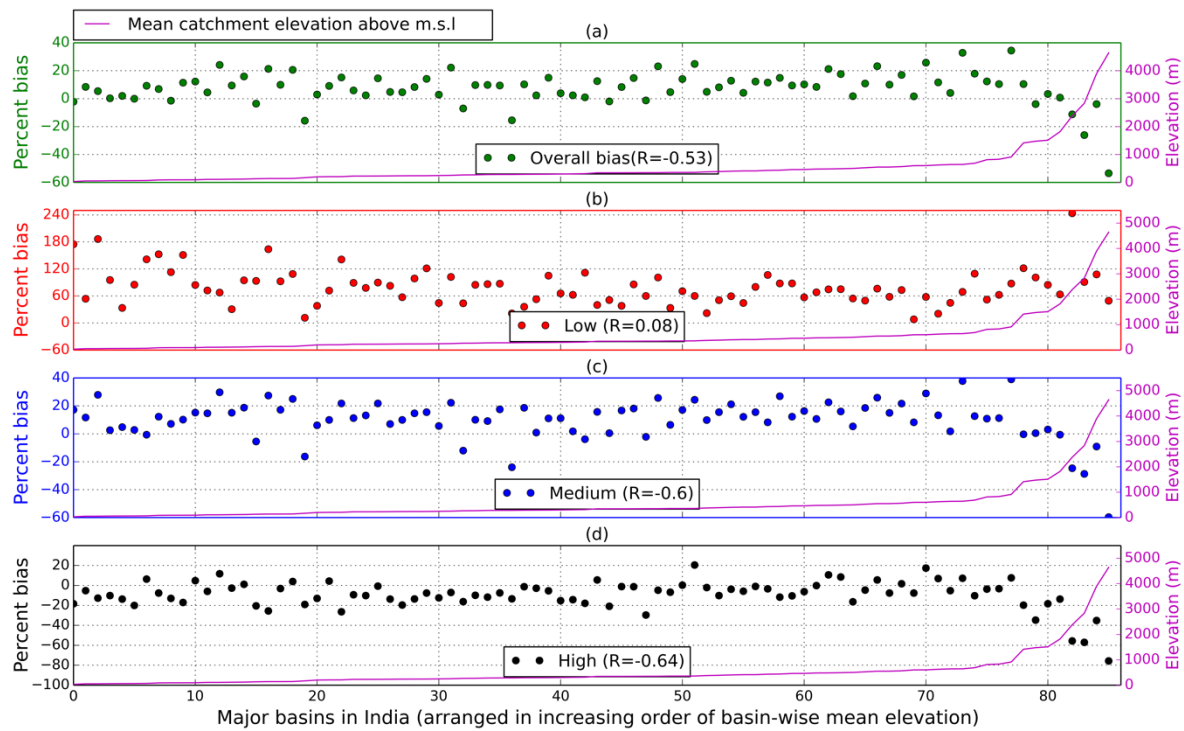


**Figure 9.** Graphical representation of percentage bias of TRMM (1998-2013) arranged in the increasing order of basin-wise average elevation over mean sea level for (a) overall time series and over (b) low, (c) medium and (d) high rainfall regime for 86 major basins in India.

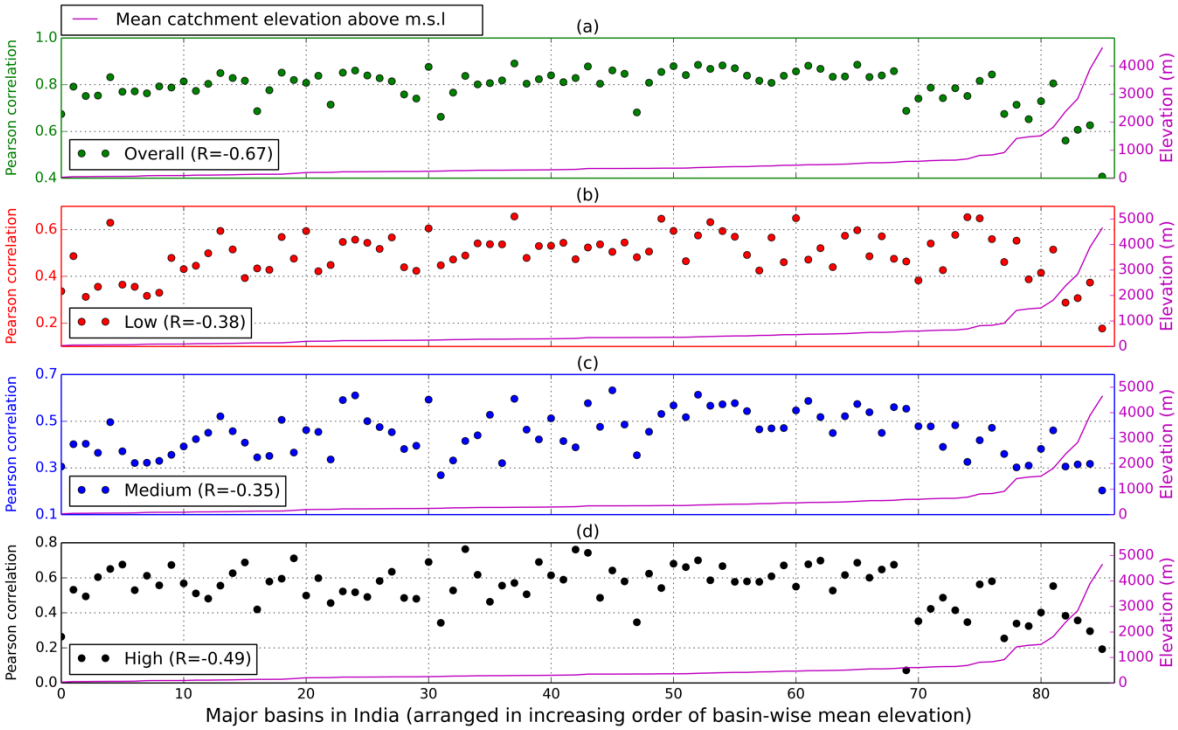


**Figure 10.** Graphical representation of correlation of TRMM (1998-2013) arranged in the increasing order of basin-wise average elevation over mean sea level for (a) overall time series and over (b) low, (c) medium and (d) high rainfall regime for 86 major basins in India.

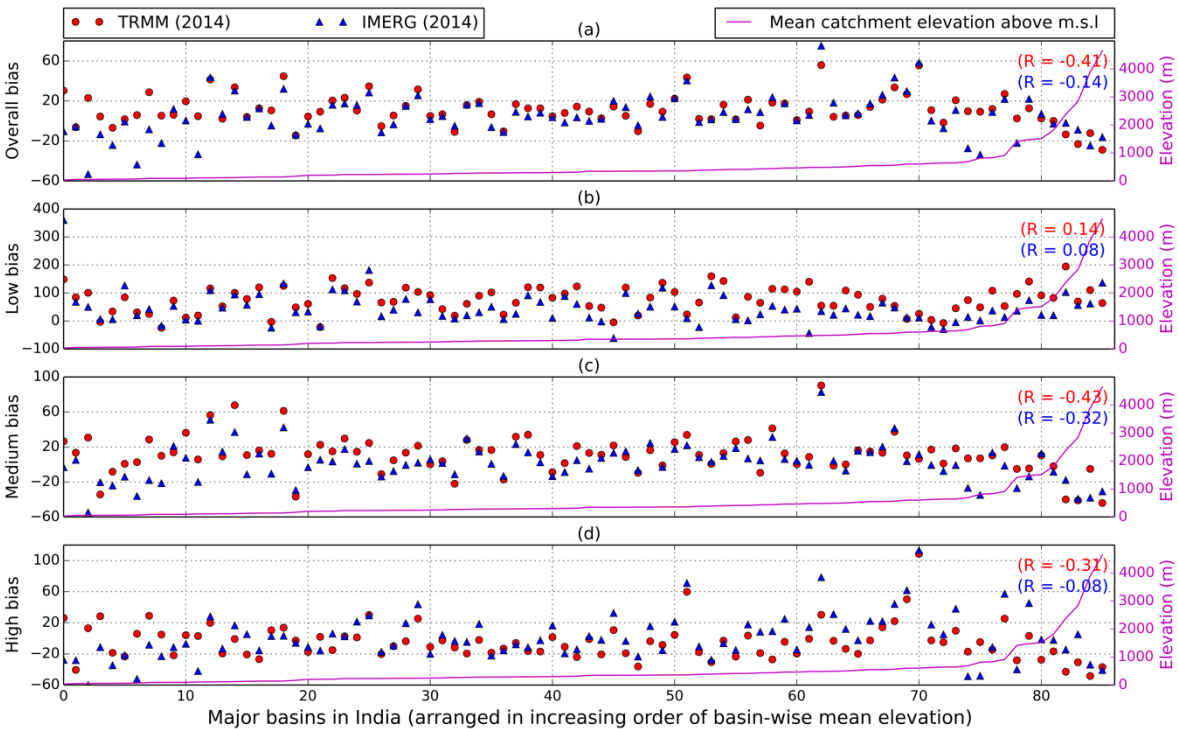


**Figure 11.** Graphical representation of percentage bias of IMERG (2014) and TRMM (2014) for 86 major basins in India.

arranged in the increasing order of basin-wise average elevation over mean sea level for (a) overall time series and over (b) low, (c) medium and (d) high rainfall regime for 86 major basins in India.

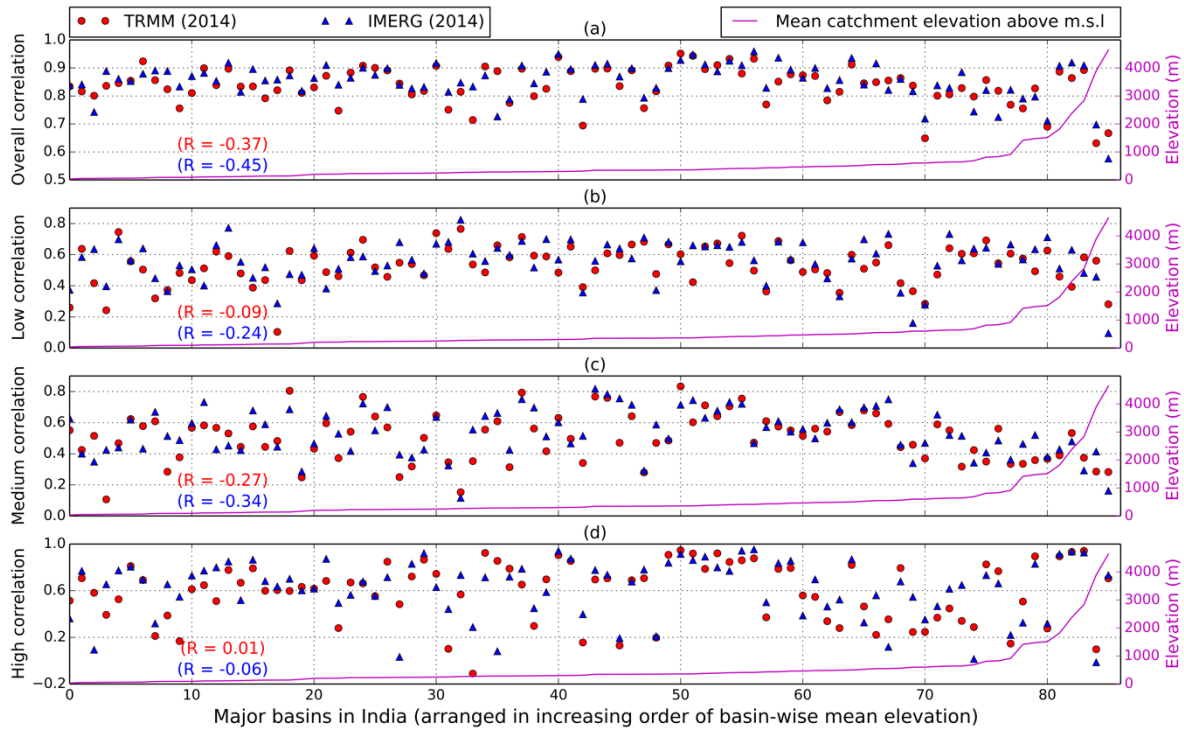


**Figure 12.** Graphical representation of correlation of IMERG (2014) and TRMM (2014) arranged in the increasing order of basin-wise average elevation over mean sea level for (a) overall time series and over (b) low, (c) medium and (d) high rainfall regime for 86 major basins in India.